Chapter 5

Indolocarbazole-benzimidazole based conjugated molecules and trisubsituted phenyl-oxazole based π-conjugated molecules: Synthesis, characterization, photophysical and DFT studies

Part a: Indolo[*3,2-b*]carbazole-benzimidazole based conjugated molecules: Synthesis, computational and photophysical studies

5.1 Introduction

Small conjugated organic molecules have been gaining quite importance recently. These molecules often show bright fluorescence in solution states and sometimes in solid states. This characteristic makes these molecules valuable due to its application in various fields from opto-electronic, electroluminescent devices and sensor devices [1].

Organic conjugated molecules possessing extended π-conjugation is one of the prime choices for the applications because of their unique photophysical properties and charges transport properties. These properties are often augmented by various strategies like setting up push-pull effect in the molecule, substitution of functional groups that enhances self assembling properties.

Indole fused with carbazole benzenoid ring form indolocarbazole heterocyclic compounds. All five isomers of indolocarbazole (ICZ) have shown remarkable application in fields of medicinal, biological and material sciences [2]. These five isomers are indolo*[2,3-b]*carbazole (1), indolo*[3,2-b]*carbazole (2), indolo*[2,3-b]*carbazole (3) and indolo*[2,3-c]*carbazole (4) and indolo*[2,3-a]*carbazole (5) which can be identified by the position and pattern of ring fusion of indole and carbazole (Figure 5.1).

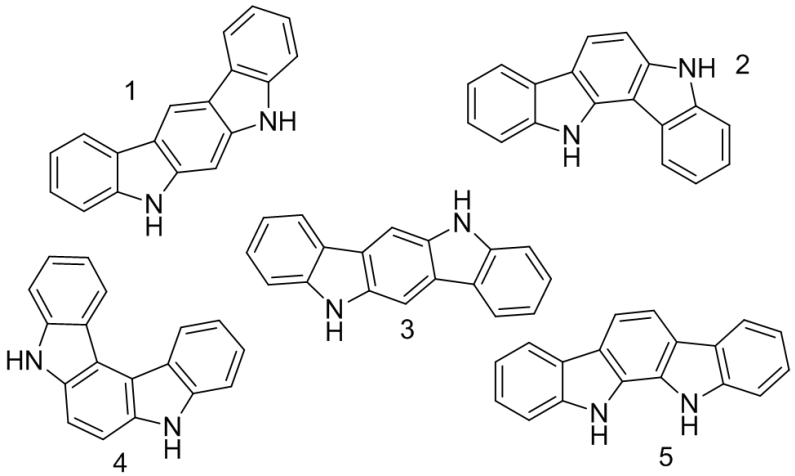

Figure 5.1 Isomers of Indolocarbazoles [1]

Among them ICZ [*3, 2-b*] derivatives have found impressive use in field of opto-electronic, non-linear optics (NLO) and as an electroluminescent devices [3]. ICZ [*3, 2-b*] derivatives possesses good photophysical properties contributed from its large rigid, planar and conjugated structure. ICZ structure is analogous to pentacene in terms of planarity, the advantages of ICZ [*3, 2-b*] are that it can be easily alkylated at $5^{th}$and 11^{th} position providing ICZ moiety better solubility in organic solvent [4]. The synthesis of ICZ [*3, 2-b*] systems have been reported in numerous ways [5]. Double fischer-cyclization reaction of bis-phenyl hydrazone yielding ICZ [*3, 2-b*] was reported by Robinson [6]. This synthetic method is quite popular even today because of its several advantages such as easy availability of starting materials, lesser synthetic steps involved etc. In present chapter, we will use similar methodology for synthesis of our desired molecules.

Benzimidazole derivatives have been widely exploited in the field of sensor especially as emissive sensor [7]. Owing to the resemblance to histidine amino acid, benzimidazole derivatives often used as model for study in biological systems [8]. Often introduction of electron withdrawing/releasing group is done to modify the pKa values of benzimidazole derivatives [9]. Recently, numerous benzimidazole derivatives have been reported as chemosensor [10], fluorescent anion receptors [11], ratiometric fluorescent acid probes [12], fluoride sensor [13] by various research groups.

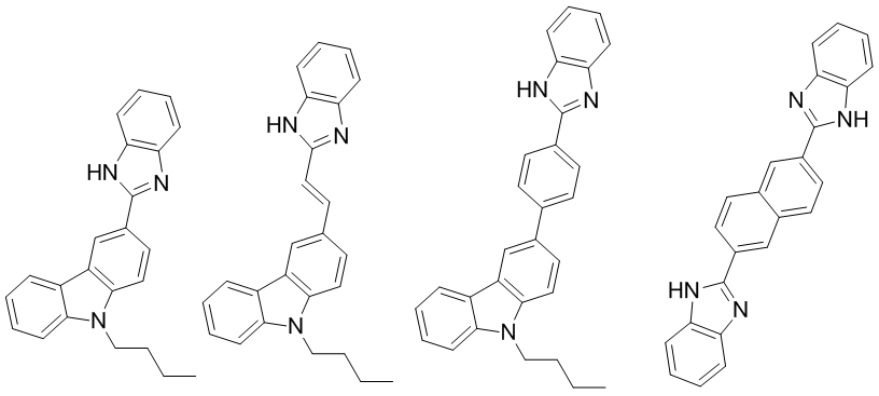

Figure 5.2 Carbazole based benzimidazole derivatives [13]

Carbazole based ratiometric fluorescent probes have been recently reported by K. Aich *et al* [14]. The reported carbazole-benzimidazole based sensor showed high and reversible sensitivity for volatile acid vapors [13]. Inherent photophysical properties of

carbazole as well as extended π-conjugation due to the presence of electron releasing and electron withdrawing groups impart unique properties to these systems. Owing to the similarity with carbazole moiety which has extensively developed as organic light emitting diode (OLED) and organic field effect transistors (OFET) devices [15].

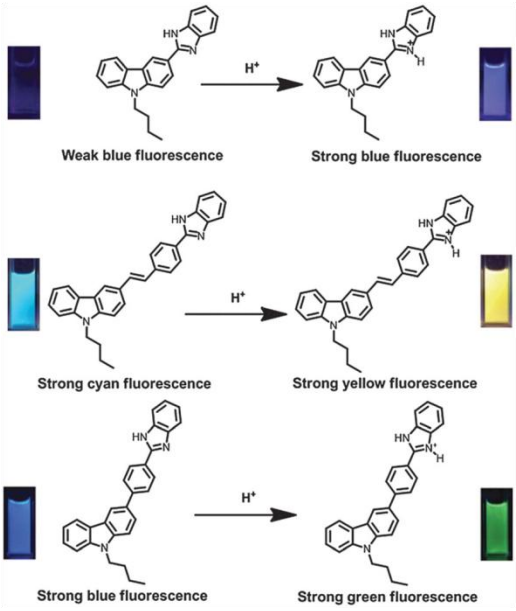

Figure 5.3 Dyes response towards H^+ acid under UV light (λ_{ex} = 365 nm) [14]

The ICZ unit possesses planar conformation which imparts certain restriction in molecular rotation as well with substitution of benzimidazole ring in the indolocarbazole-system; rigidity in these units can be enhanced. The radiationless decay of excited states results from the intramolecular vibrations can be lowered by combined effects achieved from ICZ and benzimidazole units.

In present work we reports new dialkyl ICZ-benzimidazole derivatives which were synthesized from dioctyl ICZ derivatives obtained by double Fischer cyclization of bisarylhydrazones. The dioctyl ICZ were further reacted under Vilsmeier-Haack reaction condition to yield structural isomers dioctyl ICZ-2-aldehyde and dioctyl ICZ-6-aldehyde. Both aldehydes were separately reacted with *ortho*-phenylene diamine to yield 2-(1H-benzo[d]imidazol-2-yl)-5,11-dioctyl-5,11-Indolo[*3,2-b*]carbazole (compound **5**) and6-(1H-benzo[d]imidazol-2-yl)-5,11-dioctyl-5,11-Indolo[*3,2-b*]carbazole (compound **6**). Compound **5** and compound **6** were characterized by NMR spectroscopy and High-resolution Mass-

spectrometry (HRMS). UV-visible absorption studies and fluorescence studies were analyzed. The responses of compounds against the TFA in fluorescence were measured. The computational studies were done to develop the understanding regarding acidic response by the synthesized compounds.

5.2 Result and discussion

5.2.1 Synthesis

ICZ benzimidazole compounds were synthesized as showed in the Scheme 5.1 and scheme 5.2. The ICZ moiety was synthesized by following procedure reported by Bergman *et al* [16].

ICZ were synthesized using double Fischer indolisation approach which involves reaction of the bis-phenylhydrazone with cyclohexane 1, 4-dione under condition described by Robinson [5]. The alkylation was carried out using procedure developed by Leclerc *et al*. Formylation of alkylated ICZ were performed out by following Vilsmeier-Haack conditions. The ICZ aldehydes were reacted with *ortho*-phenylene diamine in dry dimethyl formamide (DMF) in presence of *p*-TSA at elevated temperature to yield corresponding substituted benzimidazole.

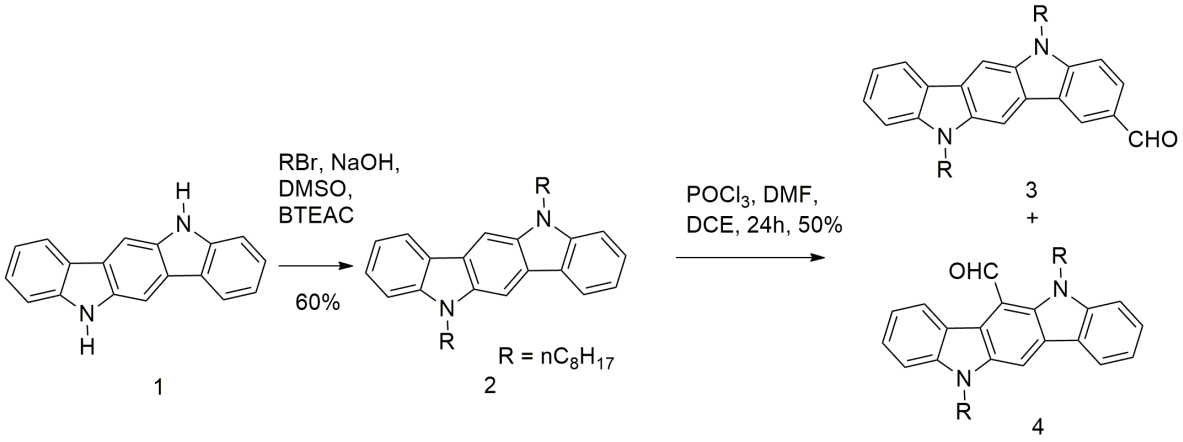

Scheme 5.1 Synthesis of dioctyl ICZ-2-aldehyde (**3**) and dioctyl ICZ-6-aldehyde (**4**) from ICZ (1)

It was observed that when compound **2** reacted with $POCl_3$/DMF under Vilsmeier-Haack conditions, two isomeric ICZ aldehydes were formed in the ratio of 70:30

(compound **4**: compound **3**). These aldehydes were separated by column chromatography. The synthesized aldehydes were used to form respective benzimidazole derivatives.

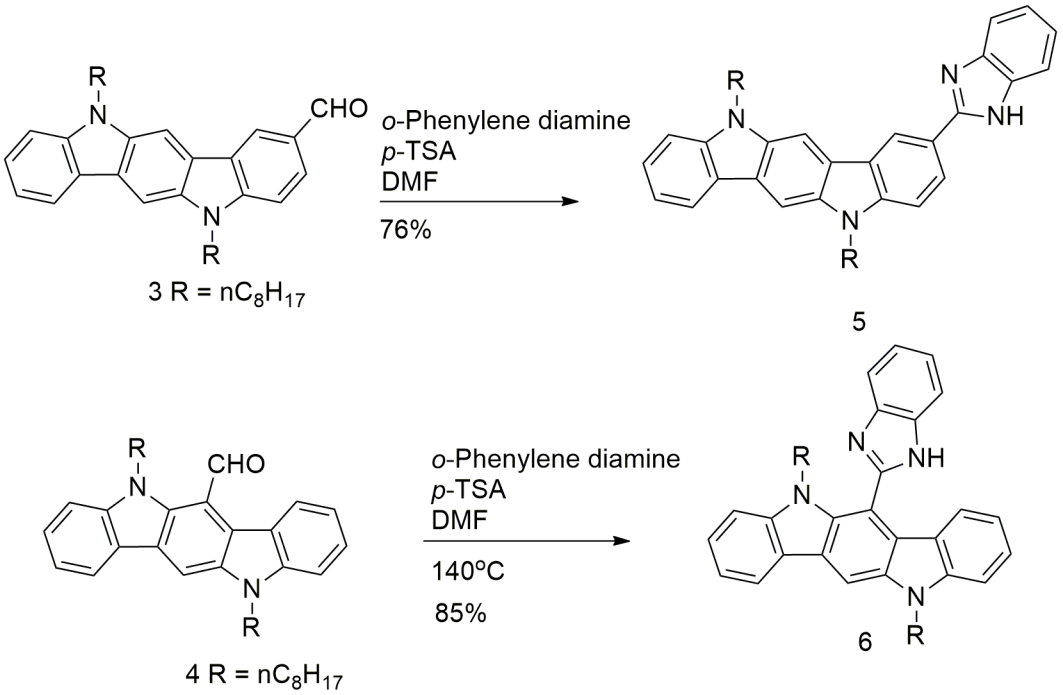

Scheme 5.2 Synthesis of 2-(*1H*-benzo[*d*]imidazol-2-yl)-5,11-dioctyl-5,11-Indolo[*3,2-b*]carbazole (**5**) and 6-(*1H*-benzo[*d*]imidazol-2-yl)-5,11-dioctyl-5,11-Indolo[*3,2-b*]carbazole (**6**) [17]

5.2.2 Photophysical properties

The UV-visible measurements of the solutions of compound were carried out. All compounds were having good solubility in organic solvents i.e methanol (MeOH), chloroform ($CHCl_3$) and acetone owing to its alkyl chains. The solutions were prepared in the MeOH with concentration in range of 10 µM. Compound **5** and compound **6** exhibited quite distinct UV-visible spectra when compared to each other. The compound **5** showed continuous spectrum where λ_{max} was observed at 343 nm which was the most intense peak. While the small humps were observed at 419 nm and at 395 nm. Compound **6** showed two clear strong peaks ranging at 341 nm and at 280 nm which was most intense. Along with these peaks small humps at 418 nm and at 395 nm were observed. A shoulder peak has been observed at 325 nm. The absorption and emission spectra of compound **5** and compound **6** are depicted in Figure 5.4.

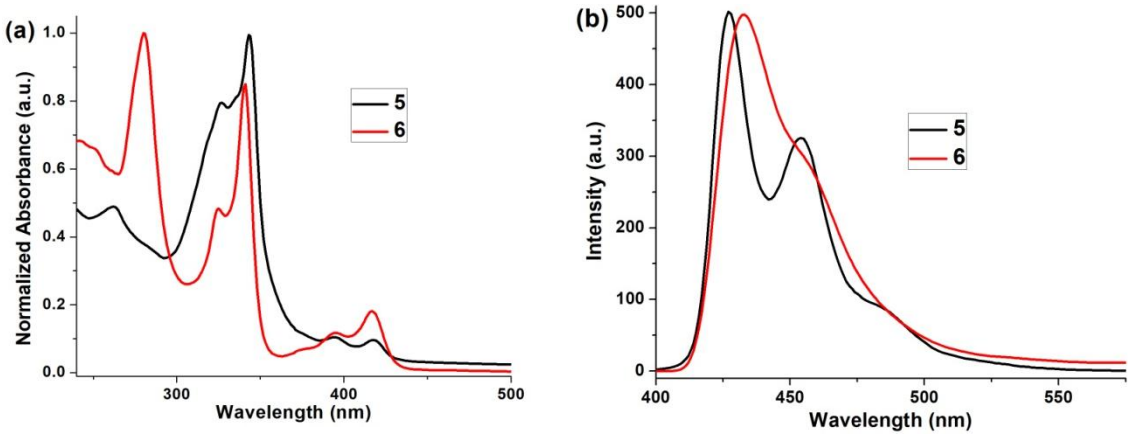

Figure. 5.4 (a) Absorption and (b) Emission spectra of compound **5** and **6** in 10 µM in MeOH

The difference in the absorption spectra of compound **5** and **6** can be attributed to the structural features. Benzimidazole substitution at 2-position in compound **5** creates less steric hindrance and in turn more conjugation compared to benzimidazole substitution at 6-position in compound **6.** In compound **6,** the benzimdiazole ring unit was substituted at 6^{th} position in the ring system which contributes much steric hindrance resulting in the twisting

of the benzimidazole ring system, this twist disrupts the conjugation across the ICZ-benzimidazole rings systems probably causing two different peaks in UV-visible spectrum.

The emissive properties of these moieties were studied. Both compound **5** and compound **6** showed different fluorescence spectrum (Figure 5.4). Compound **5** showed two distinct emission peaks, observed with intense one at 427 nm followed by second peak at 454 nm Compound **6** exhibited single peak at 433 nm. The quantum yield for the compound **5** and compound **6** were found to be 0.15 and 0.19, respectively. The colour of compound **5** solution was light yellow coloured under normal light and it appears as light blue under UV-light illumination (λ=365 nm). Compound **6** solution was colourless under normal light and under UV-illumination (λ=365 nm) shows blue-violet colour (figure 5.5).

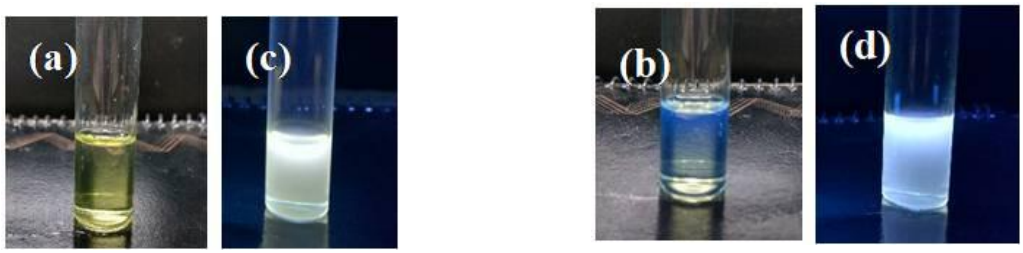

Figure 5.5 (a) Compound **5** under UV-light illumination (λ=365 nm). (b) Compound **6** under UV-light illumination (λ=365 nm)

5.2.3 Acid induced fluorescence study

Acid induced fluorescence study of both compound were examined in presence of trifluoroacetic acid (TFA).

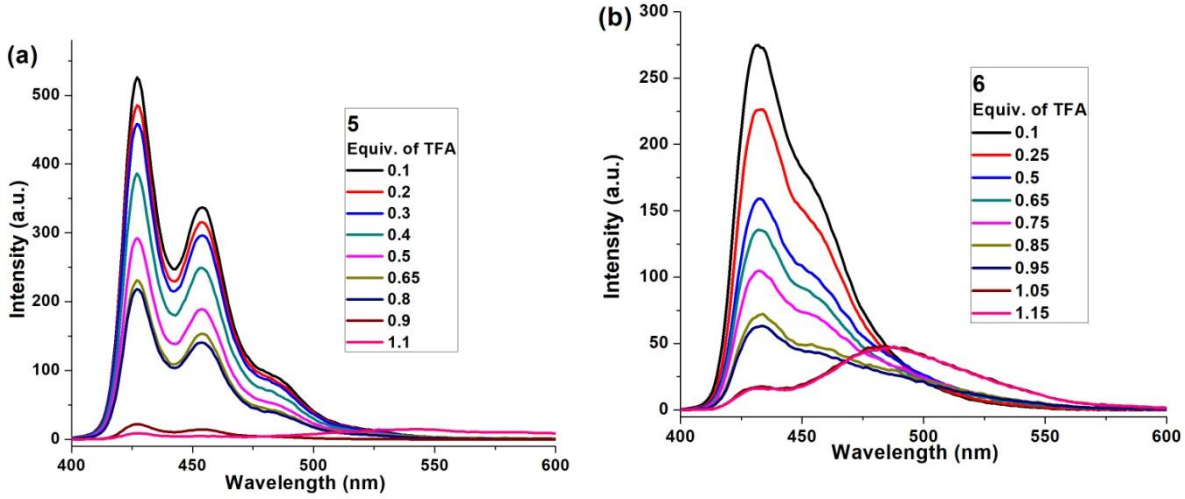

Figure 5.6 (a) Fluorescence changes of compound **5** on addition of TFA and (b) Fluorescence changes of compound **6** on addition of TFA. (λ_{ex}= 343 nm). Concentration was 10µM in MeOH solution

It was observed that with addition of TFA in the compound **5** solution, steady decrease in the emission maxima occurred and new peak at 489 nm was obtained (Figure 5.6). This red shift in the emission might be resulted from the protonation of benzimidazole nitrogen which further increasing the intramolecular charge transfer (ICT).

Similar studies were carried with compound **6**. It was observed that with addition of TFA in this compound solution, steady decrease in the emission maxima occurred and new low intensity peak at 545 nm was obtained. This red shift in the emission might be resulted from the protonation of benzimidazole nitrogen which further increasing the intramolecular charge transfer (ICT) (Figure 5.6). We have also observed similar behavior of both compound **5** and compound **6** in presence of other organic acids such as *p*-toluene sulfonic acid and trifilic acid.

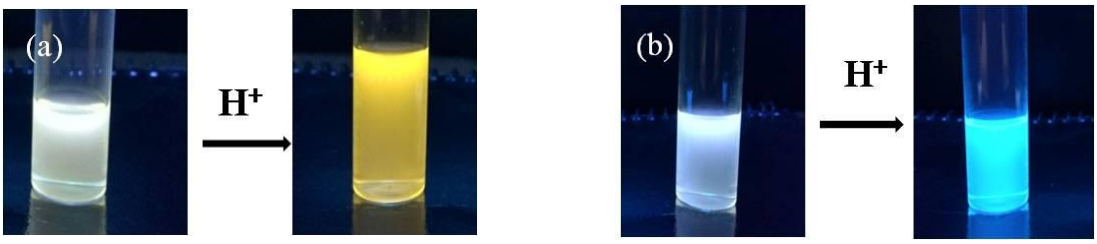

Figure 5.7 (a) Fluorescence colour change in the solution of compound **5** after TFA addition. (b) Fluorescence colour change in the solution of compound **6** after TFA addition

Fluorescence colour change upon addition of TFA in the solution of compound **5** and compound **6** were observed under UV light (λ= 365 nm). The blue violet colour of compound **6** changes to intense green-violet. Compound **5** showed change from light blue to yellow colour (Figure 5.7).

Similarly effects of acid vapors on the compound in the solid state (on TLC plates) were examined. The TLC plates which were dried after putting spots of the solution of the compound **5** and compound **6** were exposed to TFA vapors. Clear difference was observed between normal compound spot on TLC and one with TFA exposed TLC when observed under the UV-light (λ=365 nm). The colour of TFA exposed TLC returns to the normal one when it was treated to triethyl amine vapors (Figure 5.8).

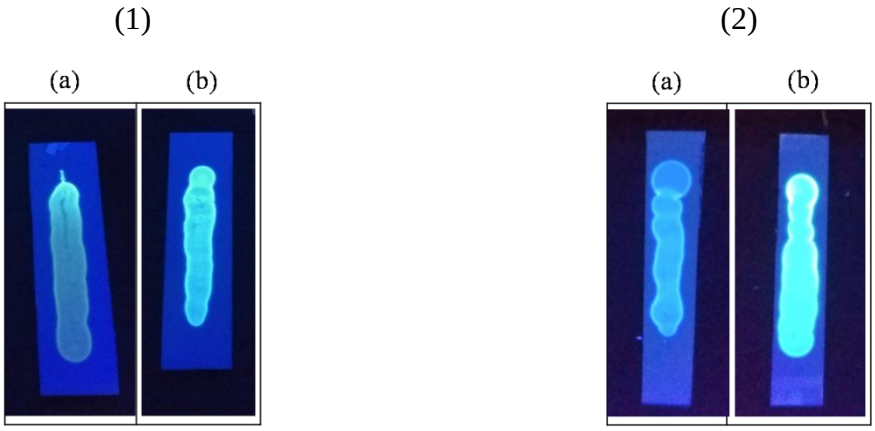

Figure 5.8 (1) (a) TLC of compound **5** under UV-light. (b) TLC of **5** after exposed to TFA vapors under UV-light. (2) (a) TLC of compound **6** under UV-light. (b) TLC of **6** after exposed to TFA vapors under UV-light

5.2.4 Electrochemical properties

Electrochemical properties of compound **5** and **6** were studied by cyclic voltammetry (CV) (Figure 5.9). The CV experiments which was employed to determine the oxidation potential of compound **5** and **6** was consists of a three-electrode cell having Pt-disk working electrode, Pt-wire counter electrode and Ag/Ag^+ reference electrode using 0.1 M tetrabutyl-ammonium hexafluorophosphate ($TBAPF_6$) as the supporting electrotye in dichloromethane (DCM) under N_2 atmosphere. Highest occupied molecular orbital (HOMO) energies of the corresponding systems were measured against the oxidation potential value observed for Ferrocene/Ferrocenium redox couple at testing condition (E_{Fc} = 0.35 V).

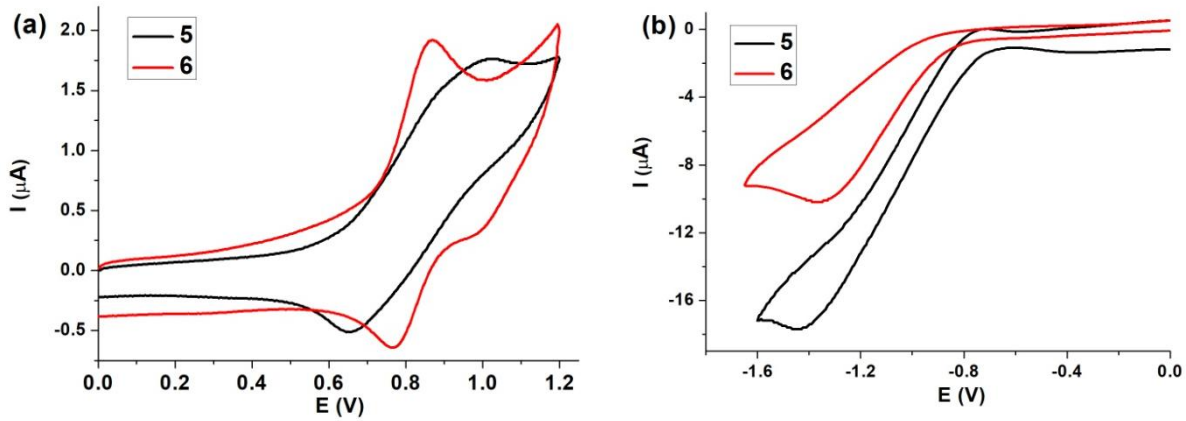

Figure 5.9 CV of compound **5** and **6**; (a) oxidation (b) reduction (vs. Ag/Ag^{+}, $E_{Fc}^{ox,onset}$= 0.36 V)

The CV of compound **5** showed quasi-reversible oxidation peak at 1.00 V with onset value of 0.68 V and irreversible reduction peak at -1.45 V with onset value of -0.70 V. The HOMO energy levels were calculated from the onset oxidation potentials. E_{HOMO} energy level of compound **5** was found to be -5.13 eV. The optical HOMO-LUMO gap of compound **5** was calculated as 2.89 eV. Lowest unoccupied molecular orbital (LUMO) energy levels were calculated from HOMO energy levels and optical HOMO-LUMO gap to be -2.24 eV. The CV of compound **6** displayed quasi-reversible oxidation peak at 0.96 V with onset value of 0.69 V and a reduction peak at -1.48 V with onset of 0.73 V. The calculated HOMO and LUMO energies were -5.14 and -2.29 eV respectively [18].

5.2.5 Computational studies

To obtain in-depth study of FMO and quantum chemical data, DFT studies were carried out using Gaussian 09 [19]. The optimization of the structures was performed using 6-31G (d) basis set with B3LYP hybrid exchange-correlation.

This computational data was used to understand probing mechanism in the ground states of molecule as well as in protonated states. These calculations also provide reasonable understanding for excitation and emission characteristics of the compounds.

The obtained optimized structure of compound **6** shows planar ICZ unit with benzimidazole unit attached in twisted fashion. The dihedral angle was calculated to be 65^{o} for compound **6** while in case of compound **5**, the attached benzimidazole unit was almost

planar to the ICZ unit with the dihedral angle of 10^{o}. It indicates that imidazole is nearly planar with ICZ in compound **5**, whereas it is highly twisted from the indolocarbazole in compound **6**.

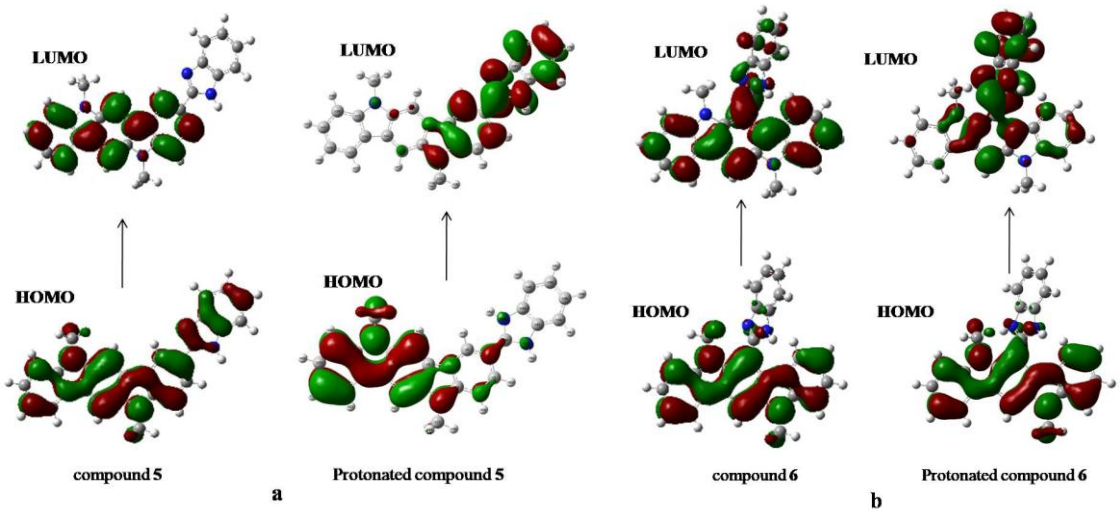

Figure 5.10 HOMO and LUMO of protonated and neutral compound (a) **5** and (b) **6**

The diminishing fluorescence response in compound **5** and **6** with addition of TFA can be understood by frontier molecular orbitals (FMO) analysis obtained from the DFT calculations (Figure. 5.10). With addition of TFA, protonation of benzimidazole unit occurs which result in the photoinduced electron transfer (PET) from fluorophore (ICZ) to positively charged benzimidazole moiety, causes quenching of fluorescence [20, 21]. PET was possible because of electron-rich ICZ moiety, which acts as electron donating moiety to the protonated benzimidazole unit during ET. For compounds **5** and **6**, the HOMO and LUMO orbitals are localized on ICZ, so there is no charge transfer (Figure 5.10). However, in case of protonated **5** and **6**, LUMO orbitals are localized on the imizazole unit, thus opening the PET channel and quenching the emission.

5.3 Conclusion

In present study, ring system consists of ICZ derivative were successfully synthesized, isolated and characterized by (^{1}H and ^{13}C) NMR spectroscopy and HRMS. Compound **3** was synthesized by new method and was used further to synthesize its

benzimidazole derivative. The synthesized compounds possessed extended conjugation which exhibited good fluorescent properties. Both the basic benzimidazole units showed sensitivity towards acid and it can be observed visually under UV-light (353 nm) with significant change in colour, glowing yellow for compound **5** and intense greenish-violet for compound **6**. Their emission spectroscopy reveals the same phenomena, where a new peak appeared at green region (490-530 nm) during protonation. The DFT studies suggested that occurrence of photoinduced electron transfer (PET) from ICZ moiety to protonated benzimidazole units results in the diminishing emission fluorescence of compound **5** and **6** with addition of TFA. Similar trend were observed with other organic acids such as trifilic acid and *p*-toluene sulfonic acid.

5.4 Experimental

5.4.1 General

All chemicals were reagent grade and were used as purchased. Moisture sensitive reactions were performed under an inert atmosphere of dry nitrogen with dried solvent. Reactions were monitored by TLC analysis using Merck silica gel 60 F-254 thin-layer plates. Column chromatography was done on Silica Gel (60-140 mesh). ^{1}H and ^{13}C NMR spectra were recorded on Bruker AV-III 400 MHz (for ^{1}H) and 100 MHz (for ^{13}C) spectrometer using $CDCl_3$/DMSO-d_6 as solvent and chemical shifts are reported in parts per million (δ scale) relative to tetramethyl silane (TMS) as the internal standard. The UV-visible spectra were recorded on model Perkin ElemerLamba 35 UV-VIS spectrometer. Fluorescence spectra were recorded on a model HITACHI F-6300 fluorescence spectrometer. The high resolution mass spectra (HRMS) were recorded on a Thermo-Fischer DSQ II GCMS instrument. Quinine was used as reference for quantum yield (Φ_s= 0.546).

5.4.2 Synthesis

ICZ (**1**) was synthesized from cyclohexane-1,4-dione *via* bishydrazone according to the literature procedure [22]. The alkylated compound (**2**) was obtained by following literature method [3].

5.4.2.1 Synthesis of 5,11-dioctyl-indolo[3,2-b]carbazole-2-carbaldehyde (3) and 5,11-dioctyl-indolo[3,2-b]carbazole-6-carbaldehyde (4) :

DMF (0.55 mL, 7.26 mmol) was taken in a clean dry two-neck round bottom flask and cooled in ice-salt bath under nitrogen atmosphere. To this $POCl_3$ (0.27 mL, 2.9 mmol) was added and the mixture was stirred at 0^{o} C for 30 minutes and then at room temperature for 1 hour. Compound **2** (0.7 g, 1.45 mmol) was dissolved in dichloroethane (DCE) (15 mL) and kept under nitrogen atmosphere. The $POCl_3$ in DMF was cooled to 0^{o} C and to this mixture solution of compound **2** in DCE was added dropwise with the help of syringe.

Reaction mixture was stirred at room temperature for 1 hour and then refluxed (85^{o} C) for 24 hours. After completion of reaction, DCE was evaporated and the remaining mass was stirred with water (30 mL) and then extracted with DCM (3 x 15 mL). The combined organic layer was washed with brine and then dried over anhydrous Na_2SO_4. After evaporating solvent under reduced pressure, the crude products were subjected to alumina column chromatography and two products compound **3** (EA/PE: 05/95) and compound **4** were separated (EA/PE: 15/85). Compound **3** was obtained in 30% yield (0.370 g) M.P.: 132 ^{o}C. and compound **4** was obtained in 50% yield (0.207 g) M.P.: 102 ^{o}C.

Compound 3 ***^{1}H NMR*** *(400 MHz, $CDCl_3$, ppm): δ* 0.86-0.89 (m, 6H), 1.25-1.42 (m, 20H), 1.87-1.94 (m, 4H), 4.33-4.37 (t, 4H, J=7.2 Hz), 7.33-7.37 (m, 1H), 7.47-7.51) (m, 3H), 7.54-7.58 (m, 1H), 8.02-8.04 (dd, 1H, J_1=8.8 Hz, J_2=1.6 Hz), 8.17-8.19 (d, 2H, J=8 Hz), 8.63 (d, 1H, J=1.2 Hz), 10.12 (s, 1H).

^{13}C NMR *(100 MHz, $CDCl_3$, ppm): δ* 14.08, 22.62, 27.36, 27.45, 28.81, 28.87, 29.20, 29.24, 29.39, 29.47, 31.81, 31.84, 43.44, 43.64, 99.29, 99.62, 108.44, 108.60, 118.24, 120.34, 122.54, 122.60, 123.21, 123.39, 123.50, 126.15, 127.66, 136.31, 136.68, 141.78, 145.23, 191.73.

Compound 4 ***^{1}H NMR*** *(400 MHz, $CDCl_3$, ppm): δ* 0.85-0.89 (m, 6H), 1.26-1.48 (m, 20H), 1.81-1.85 (m, 2H), 1.93-1.97 (m, 2H), 4.44-4.48 (t, 2H, J=7.2 Hz), 4.57-4.60 (t, 2H, J=8 Hz), 7.26-7.28 (m, 2H), 7.30-7.35 (m, 1H), 7.48-7.59 (m, 4H), 8.21-8.23 (d, 1H, 7.6 Hz), 8.29 (s, 1H), 8.64-8.66 (d, 1H, J=8 Hz), 11.36 (s, 1H).

^{13}C NMR *(100 MHz, $CDCl_3$, ppm)*: *δ* 14.14, 22.65, 26.82, 27.40, 28.72, 28.96, 29.24, 29.45, 31.79, 31.85, 43.15, 47.29, 105.43, 108.7, 109.83, 115.94, 11.82, 119.55, 121.67, 122.21, 122.64, 124.85, 125.41, 126.64, 135.62, 136.01, 190.36.

5.4.2.2 Synthesis of 2-(1H-benzo[d]imidazol-2-yl)-5, 11-dioctyl-indolo[3,2-*b*]carbazole(5)

A mixture of compound **3** (0.330 g, 0.647 mmol) and *o*-phenylene diamine (0.167 g, 1.55 mmol) was dissolved in DMF (5 mL) and *p*-TSA was added in catalytic amount (0.020 g). The reaction mixture was refluxed (155 ^{o}C) under nitrogen atmosphere for 12 hours. The reaction mixture was cooled to room temperature and then it was poured into ice water (30 mL) and stirred for some time which is then extracted with DCM (3 x 15 mL). The combined organic layer was washed first with water and then with brine twice and then it was dried over anhydrous Na_2SO_4. The solvent was evaporated under reduced pressure and the crude product was purified by alumina column chromatography (EA/PE: 05/95). Compound **5** was obtained as yellow solid in 85 % yield (0.328 g). M.P.: 166 ^{o}C

IR (KBr) (*cm*$^{-1}$): *v* 3068, 2952, 2852, 1616, 1509, 1467, 1441, 1403, 1310, 1273, 1223, 1174, 1147, 1073, 844, 743.

^{1}H NMR *(400 MHz, $CDCl_3$, ppm):* δ 0.84-0.87 (m, 6H), 1.24-1.40 (m, 22H), 1.88-1.91 (m, 4H), 4.29-4.30 (m, 4H), 7.23-7.25 (m, 1H), 7.27-7.29 (m, 1H), 7.35-7.42 (m, 2H), 7.49-7.53 (m, 1H), 7.70 (s, 1H), 7.95-7.98 (d, 2H), 8.08-8.10 (d, 1H), 8.19-8.21 (d, 1H), 9.03 (s, 1H).

^{13}C NMR *(100 MHz, $CDCl_3$, ppm):* δ 14.12, 22.61, 22.64, 27.26, 28.62, 28.83, 29.19, 29.26, 29.32, 29.59, 31.81, 31.91, 42.66, 42.97, 98.76, 108.49, 114.86, 117.79, 119.25, 119.41, 120.09, 122.22, 122.56, 122.61, 122.85, 123.36, 124.15, 125.63, 135.85, 136.00, 141.45, 142.29.

HRMS: Calculated for $C_{41}H_{48}N_4$ $(M+1)^+$ (m/z): 596.3879. Found: 597.3960

5.4.2.3 Synthesis of 6-(*1H*-benzo[d]imidazol-2-yl)-5,11-dioctyl-indolo[*3,2-b*]carbazole (6)

A mixture of compound **4** (0.180 g, 0.353 mmol) and *o*-phenylene diamine (0.91 g, 0.85 mmol) was dissolved in DMF (5 mL) and *p*-TSA was added in catalytic amount (0.020 g). The reaction mixture was refluxed (155 ^{o}C) under nitrogen atmosphere for 12 hours. The reaction mixture was cooled to room temperature, and then it was poured into ice water (30 mL) and stirred for some time which was then extracted with DCM (3 x 15 mL). The

combined organic layer was washed first with water and then with brine twice and then it was dried over anhydrous Na_2SO_4. The solvent was evaporated under reduced pressure and the crude product was purified by alumina column chromatography (EA/PE: 05/95). Compound **6** was obtained as yellow solid in 46% yield (0.096 g). M.P.: 181 ^oC

IR (KBr) (*cm^{-1}*): *v* 3063, 2925, 2853, 1613, 1586, 1537, 1506, 1471, 1453, 1417, 1370, 1277, 1225, 1176, 1122, 1092, 841, 738.

^{1}H NMR *(400 MHz, $CDCl_3$, ppm):* δ 0.47- 0.49 (m , 3H), 0.64-0.68 (m, 3H), 0.86-1.01 (m, 8H), 1.15-1.40 (m, 15H), 1.85-1.88 (m, 2H), 4.26 (m, 4H), 6.53-6.55 (d, 1H), 6.79 (m, 1H), 7.12-7.14 (m, 1H), 7.26-7.30 (m, 2H), 7.33-7.34 (m, 1H), 7.46-7.53(m, 2H), 7.84 (s, 1H), 8.16-8.18 (d, 1H).

^{13}C NMR *(100 MHz, $CDCl_3$, ppm)*: δ 14.15, 14.18, 22.63, 22.68, 26.63, 27.35, 28.70, 29.19, 29.28, 29.44, 31.64, 31.90, 43.03, 44.45, 100.54, 108.22, 108.75, 118.35, 119.98, 121.11, 122.29, 122.34, 123.14, 123.46, 125.71, 126.00, 133.97, 134.67, 141.45, 142.18, 148.75.

HRMS: Calculated for $C_{41}H_{48}N_4$ $(M+1)^+$ (m/z): 596.3879. Found: 597.3980.

5.5 Spectral data

5.5.1 5, 11-di-n-octyl indolo[*3,2-b*] carbazole (2)

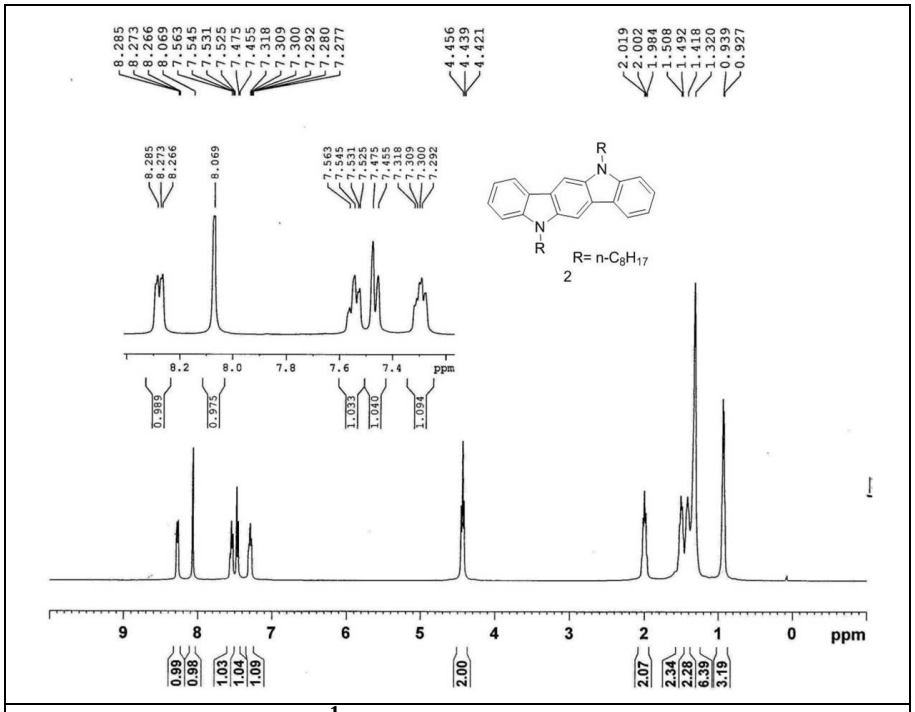

^{1}H NMR spectrum

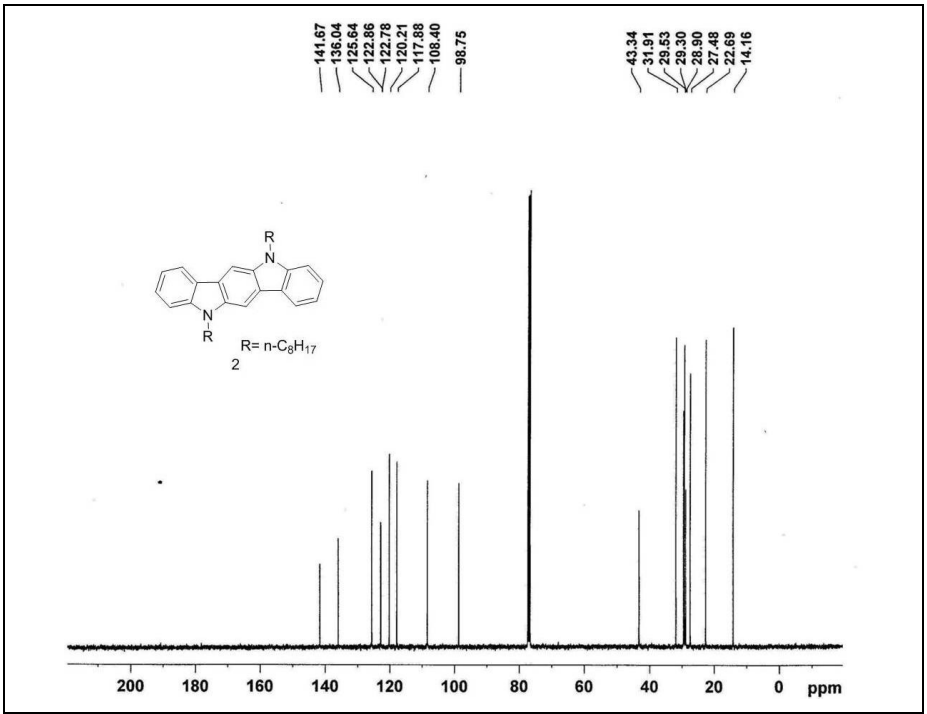

^{13}C NMR spectrum

5.5.2 5,11-dioctyl-indolo[*3,2-b*]carbazole-2-carbaldehyde (3)

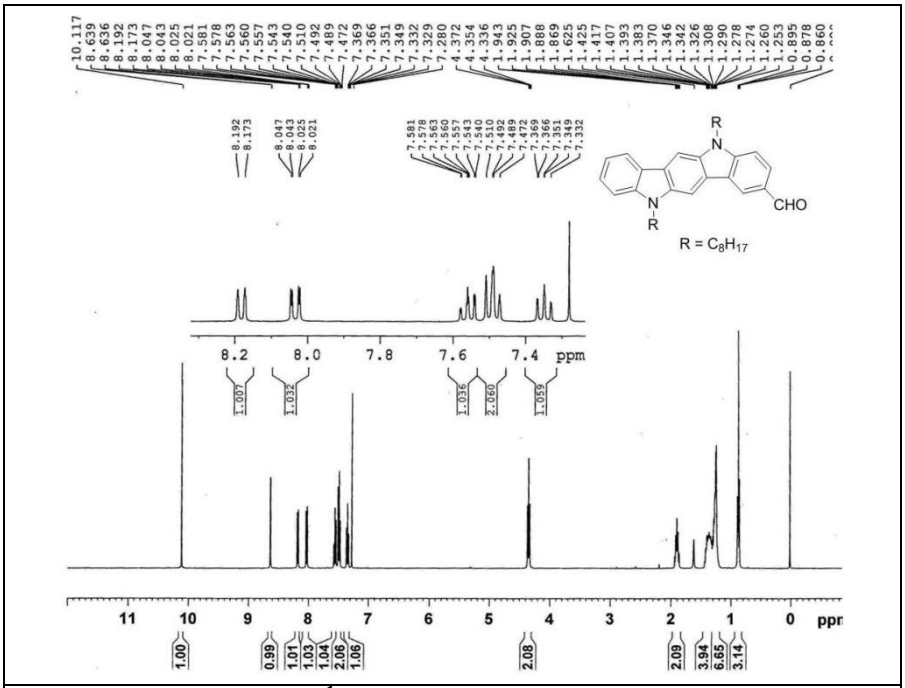

^{1}H NMR spectrum

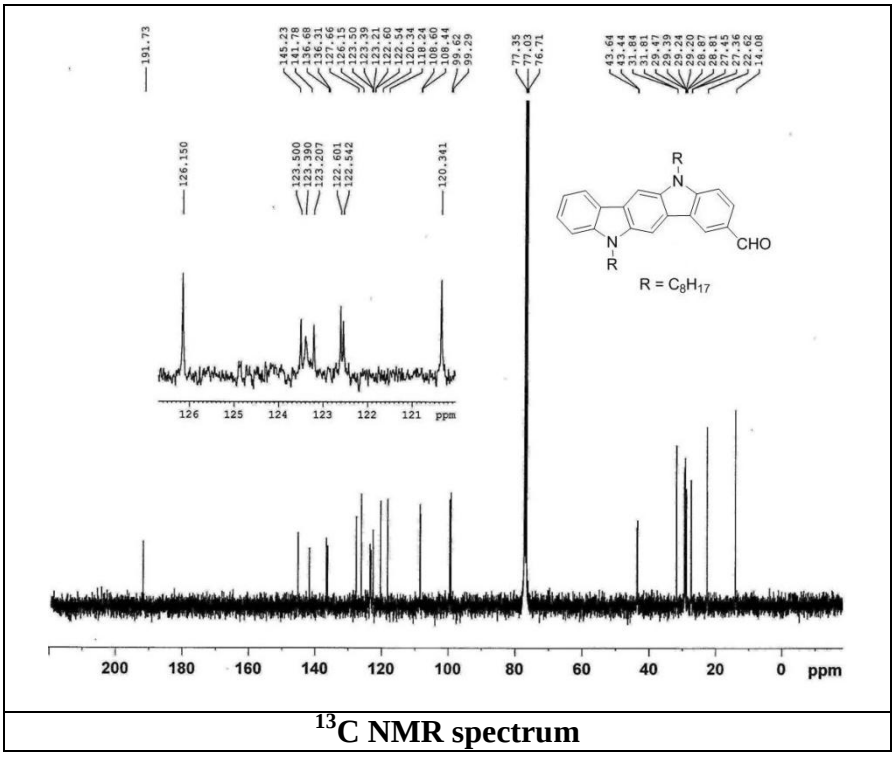

^{13}C NMR spectrum

5.5.3 5,11-dioctyl-indolo[*3,2-b*]carbazole-6-carbaldehyde (4)

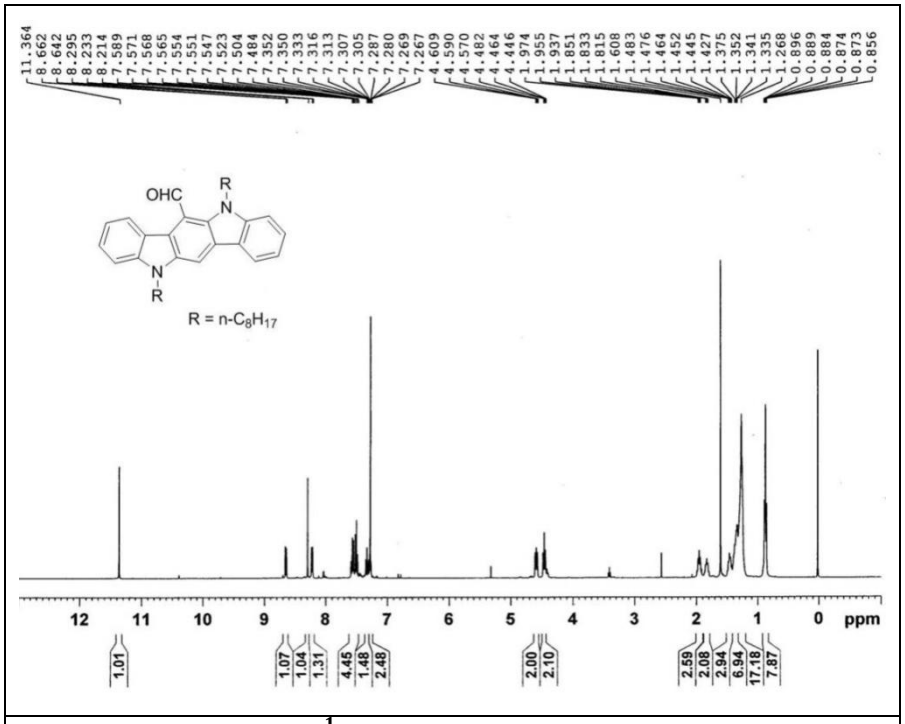

^{1}H NMR spectrum

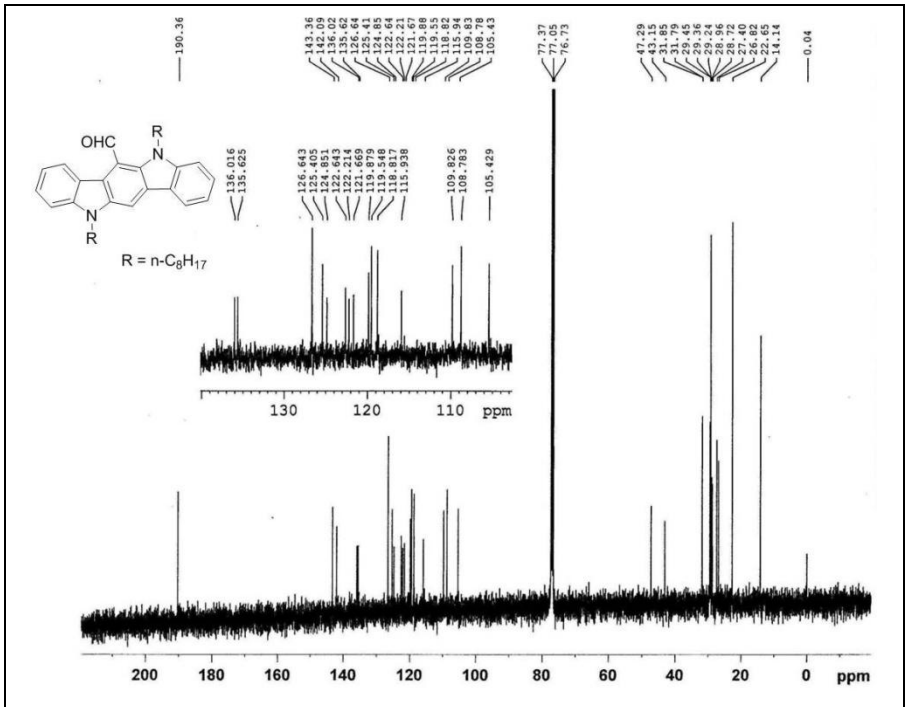

^{13}C NMR spectrum

5.5.4 2-(1H-benzo[*d*]imidazol-2-yl)-5, 11-dioctyl-indolo[*3,2-b*]carbazole (5)

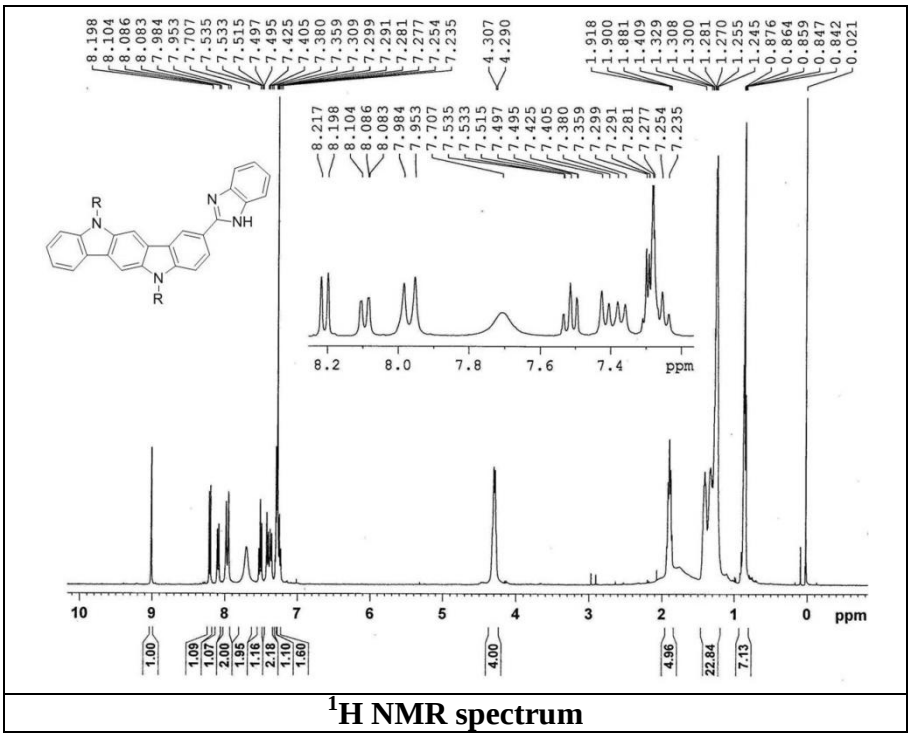

^{1}H NMR spectrum

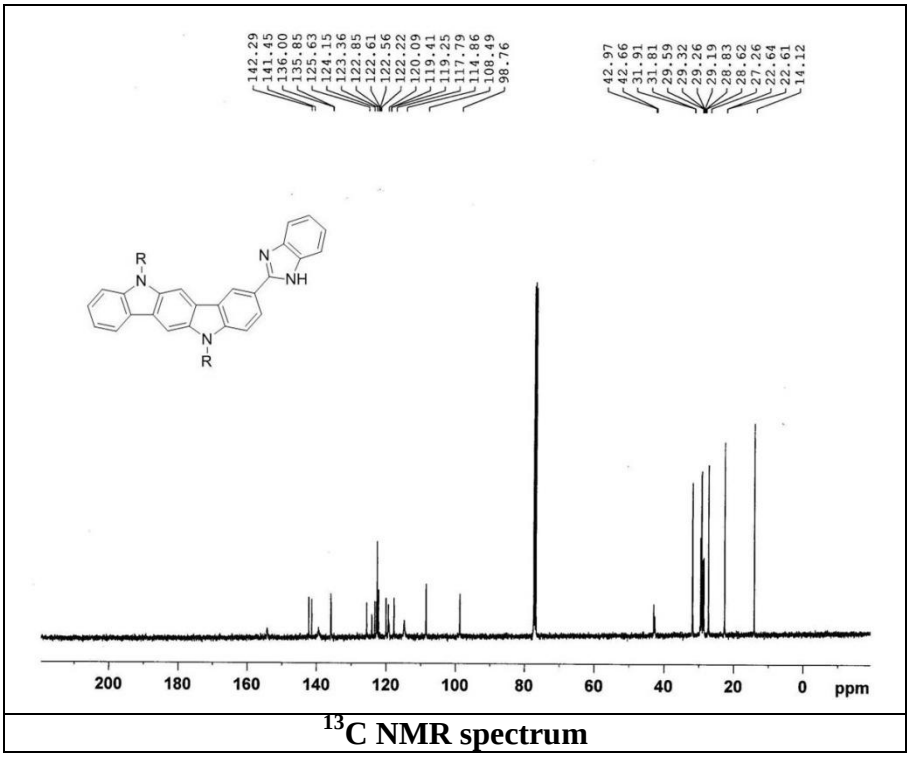

^{13}C NMR spectrum

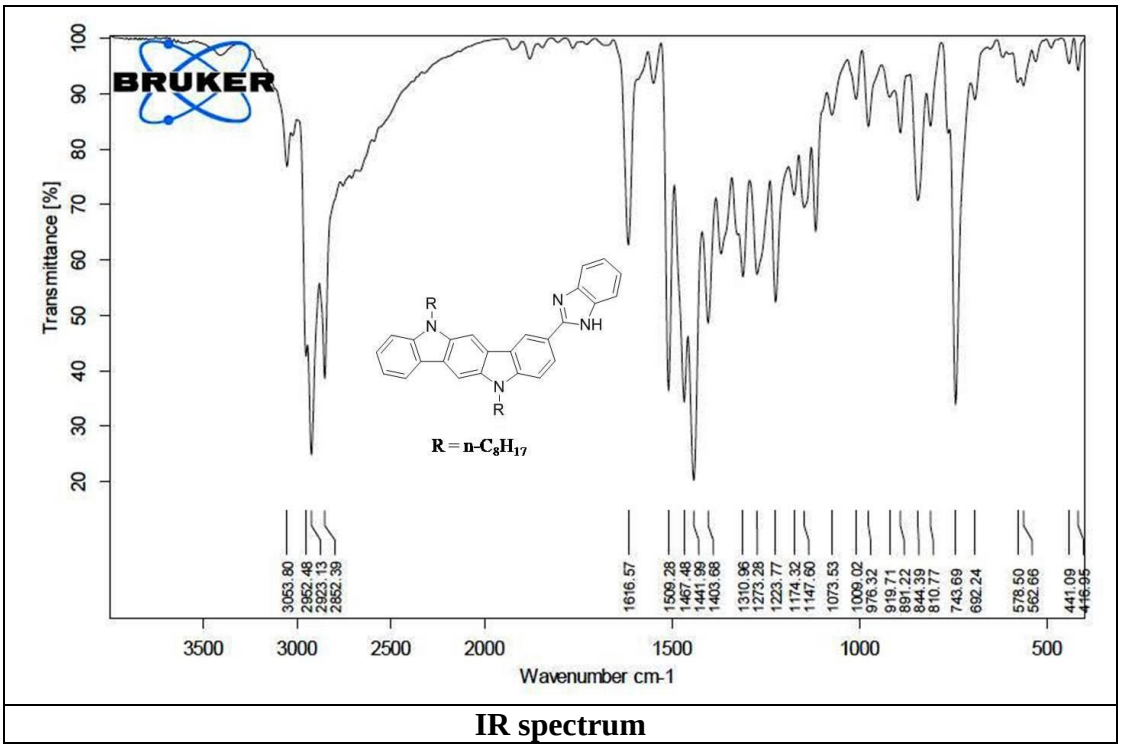

IR spectrum

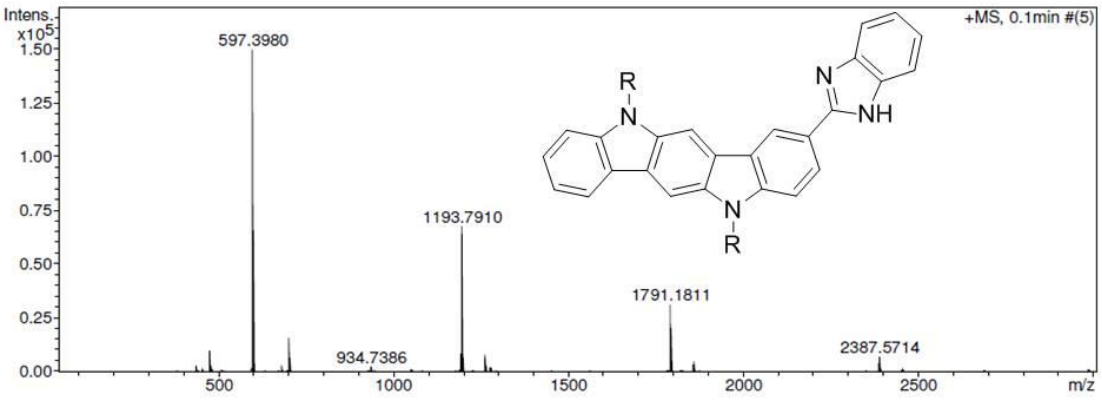

HRMS

5.5.5 6-(1H-benzo[*d*]imidazol-2-yl)-5,11-dioctyl-indolo[*3,2-b*]carbazole (6)

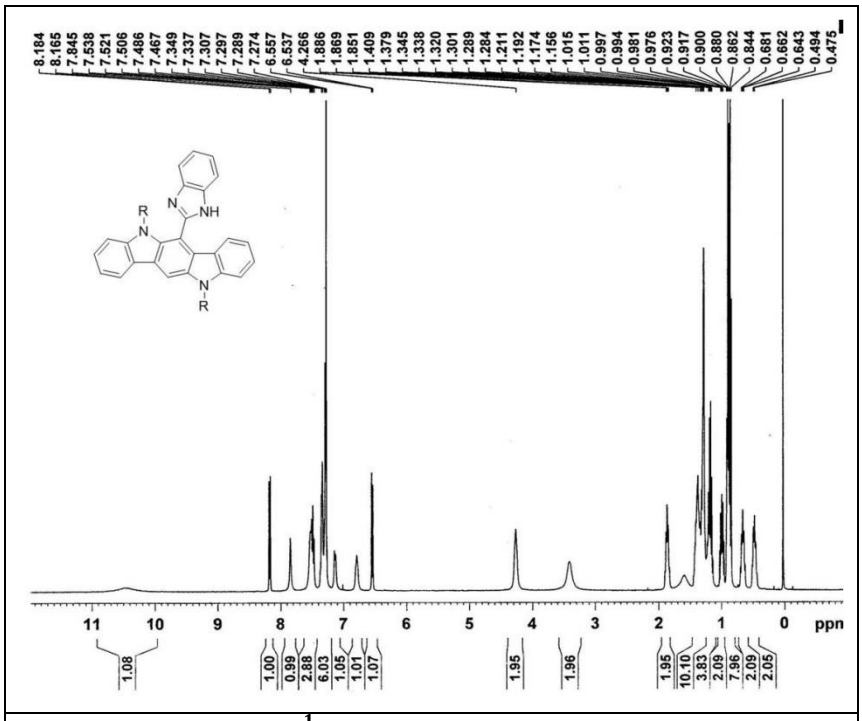

^{1}H NMR spectrum

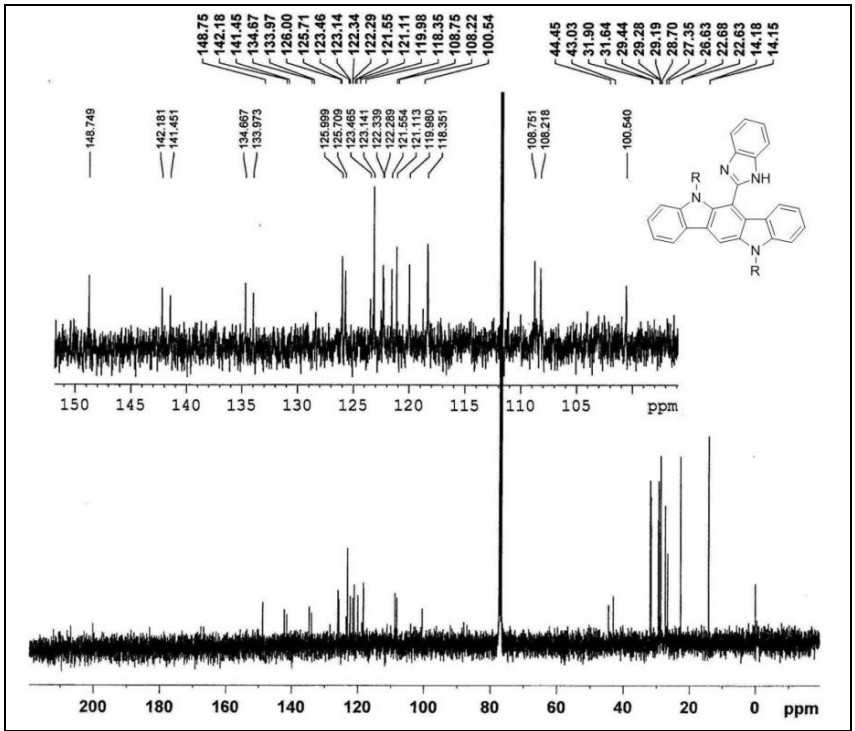

^{13}C NMR spectrum

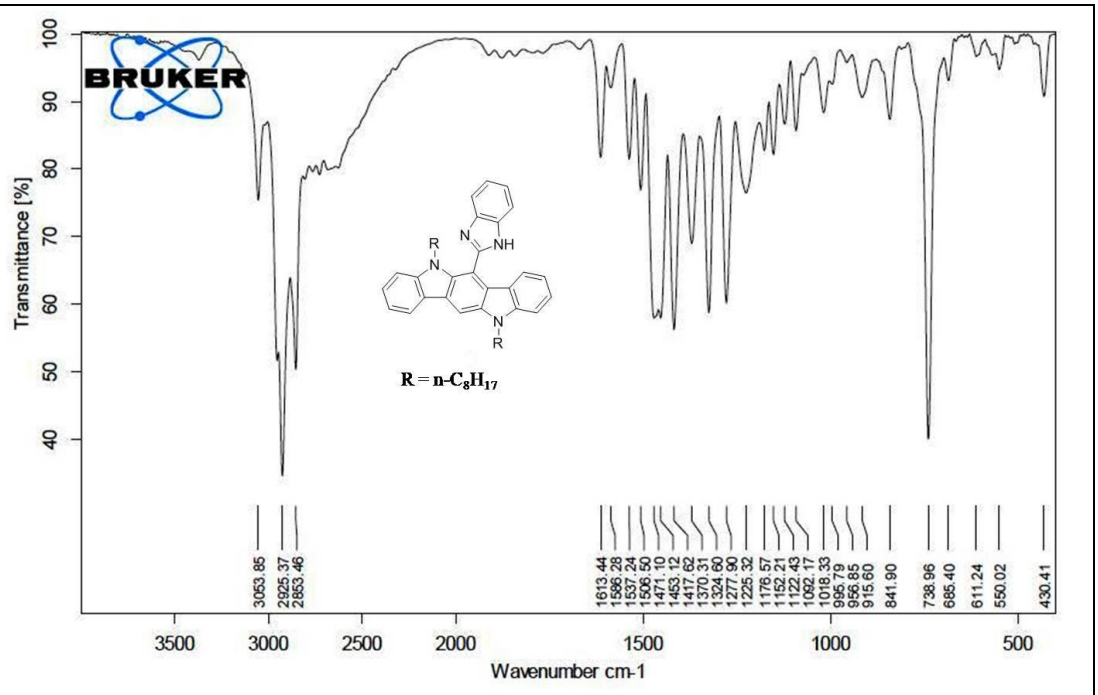

IR spectrum

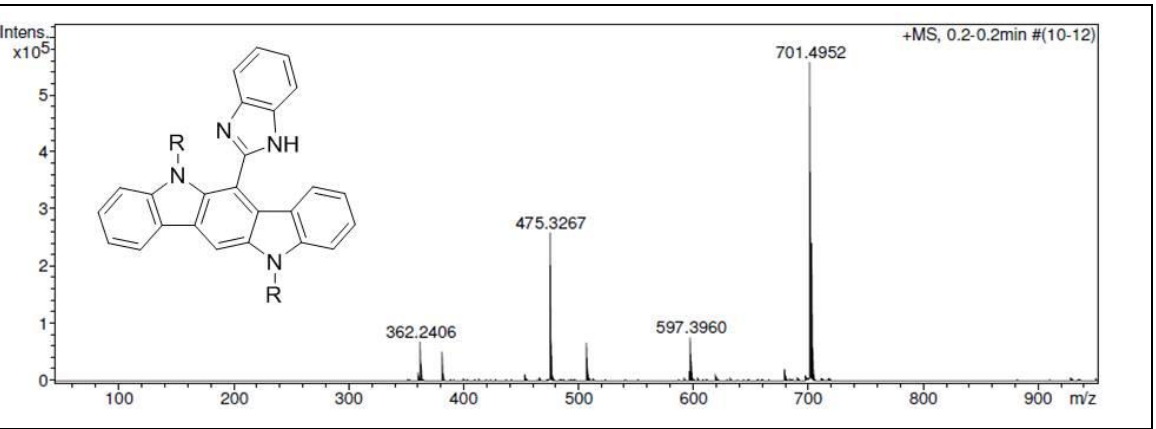

HRMS

Chapter 5

Indolocarbazole-benzimidazole based conjugated molecules and trisubsituted phenyl-oxazole based π-conjugated molecules: Synthesis, characterization, photophysical and DFT studies

Part b: Series of 2, 4, 5-trisubstituted oxazole: Synthesis, characterization and DFT studies

5.6 Introduction

Azoles are a class of five-membered ring, heteroaromatic compounds, isoconjugate with the cyclopentadienyl anion and derived from this species by replacing two of the carbons with a nitrogen atom and another heteroatom [23]. 1, 3-azoles-oxazoles, thiazoles, imidazoles, have attracted the attention of chemists for many years. Imidazole-, oxazole- and thiazole-containing secondary metabolites are extensively distributed in nature, both in marine and terrestrial organisms [24]. Oxazole has an oxygen atom and a nitrogen atom at the 1 and 3 positions of the ring, and, like pyridines, oxazoles are weakly basic substances [25].

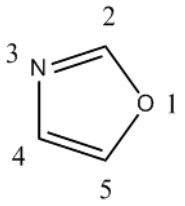

Figure 5.11 Structure of oxazole

Oxazoles have been found as subunits in numerous natural products [26]. Oxazole is also a valuable precursor in various biochemical as well as synthetic transformations [27]. Numerous pharmacologically important compounds used as antibiotics and antiproliferatives contain oxazole ring systems. Some very important derivatives of 2,5-diaryloxazoles, such as annuloline (from Loliummultiflorum) [28] and halfordinol (from Halfordiascleroxyla) [29] have been isolated from plant sources and have also been prepared in the laboratories. Annuloline was the first demonstration of the oxazole ring in nature.

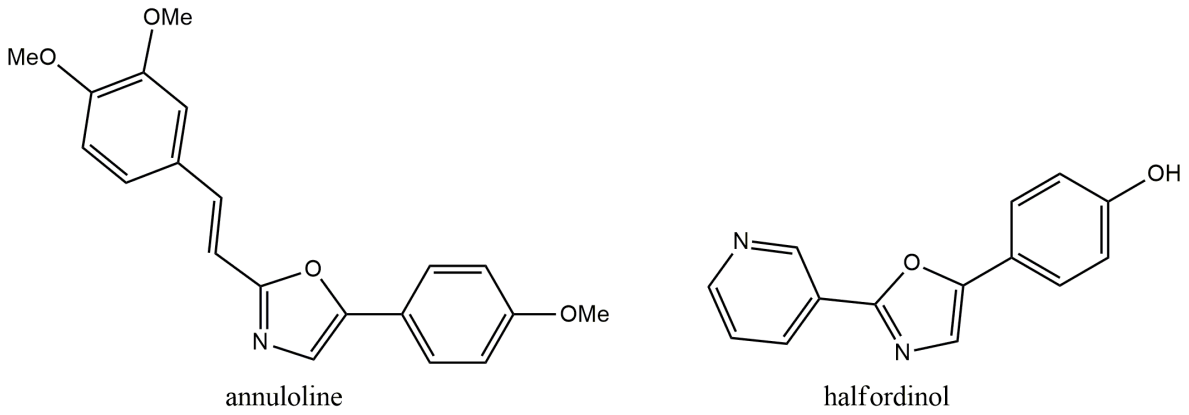

Figure 5.12 Structures of annuloline and halfordinol

Oxazole ring containing pimprinine (a mould metabolite from Streptomyces pimprina) acts as antibiotics. Several methods for the synthesis of pimprinine have been reported [30].

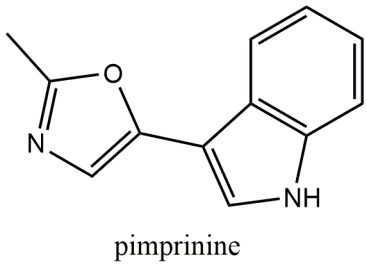

Figure 5.13 Structure of Pimprinine

Among the numerous heterocyclic moieties of biological and pharmacological interest, the oxazole ring is endowed with various activities. Oxazole derivatives have shown activity against inflammation [31], diabetes [32], bacterial infection [33], cardiovascular disease [34], viral [35] and cancer [36]. Owing to these facts, oxazole derivatives have attracted considerable attention in field of medicinal research, and resulted in development of numerous investigations on their synthesis and biological activities during the last decade. However, very little efforts have been paid to the synthesis of trisubstituted oxazoles.

Earliest synthesis to produce 2, 5-disubstituted oxazoles was reported by Hermann Emil Fischer in 1896. It is a type of dehydration reaction which involves preparation of oxazole from cyanohydrins and aldehydes in the presence of anhydrous HCl [21]. Oxazoles

have been synthesized by various method utilizing α-diazo ketones, α-acyloxy ketones and α-acylamino ketones as synthetic intermediates. However, preparation of these reactive intermediates is not always straightforward because of various drawbacks involved in these reactions, such as long reaction time, low yields, and forced reaction conditions [21]. Bredereck and Bangert showed a relatively simple approach to the synthesis of oxazoles (Scheme 5.3) [37]. This method was an adaptation of an older synthesis of substituted oxazoles, which was the reaction of amides with α-hydroxy ketones. Upon heating formamide with ethyl α-hydroxyketosuccinate, diethyl oxazole-4,5-dicarboxylate was obtained.

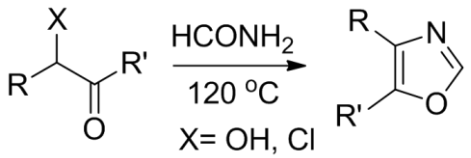

Scheme 5.3 Synthesis of disubsituted oxazoles reported by Bredereck [35]

In present chapter we will be using modified Bredereck method for synthesis of 2-(4-alkyloxyphenyl)-4,5-dimethyloxazole derivatives and other trisubsituted oxazole derivatives. A simple and practical synthetic methodology was used to achieve the desired molecules. These compounds were thoroughly characterized by IR, NMR (^{1}H and ^{13}C). The structures of representative compounds were determined by single crystal X-ray diffraction. Density Functional Theory (DFT) calculations were performed to shed more light on the electronic structures of these molecules [38].

5.7 Results and discussion

5.7.1 Synthesis

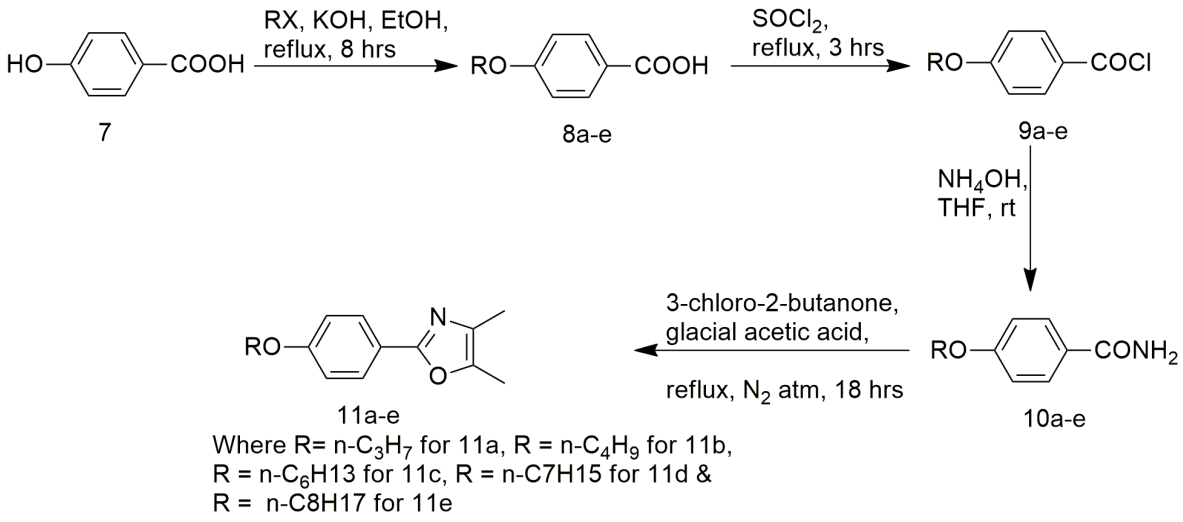

Scheme 5.4 Synthesis of 2-(4-alkyloxyphenyl)-4, 5-dimethyloxazole derivatives (**11a-e**) [39]

2-(4-Alkyloxyphenyl)-4,5-dimethyloxazole derivatives (**11a-e**) were synthesized by the procedures shown in the scheme 5.4 using the modified Bredereck method. Treatment of 4-hydroxy benzoic acid with appropriate alkyl halides in presence of alcoholic KOH has afforded 4-alkoxybenzoic acids (**8a-e**) in 80-90%. Compounds **9** were obtained in good yield by treatment of compounds **8** with thionyl chloride at reflux temperature and followed by treatment with ammonium hydroxide in THF at room temperature to yield corresponding compound **10**.

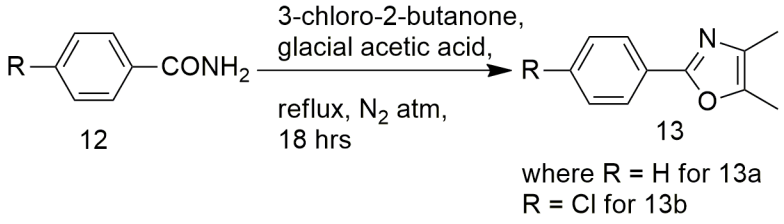

Scheme 5.5 Synthesis of 4, 5-dimethyl-2-phenyloxazole (**13a**) and 2-(4-chlorophenyl)-4,5-dimethyloxazole (**13b**)

4,5-Dimethyl-2-phenyloxazole (**13a**) was synthesized from benzamide by refluxing with 3-chloro-2-butanone in glacial acetic acid (Scheme 5.5).

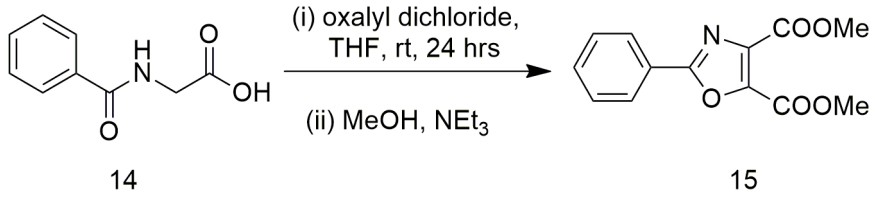

Scheme 5.6 Synthesis of dimethyl-2-phenyloxazole-4, 5-dicarboxylate (**15**)

Moreover, dimethyl-2-phenyloxazole-4, 5-dicarboxylate (**15**) was also prepared by treating N-benzoyl glycine (**14**) with oxalyldichloride in dry THF under nitrogen atmosphere followed by treatment with methanol in presence of triethyl amine (Scheme 5.6) [40].

5.7.2 Single crystal X-ray Diffraction (SCXRD)

The molecular structures for 2-(4-butyloxyphenyl)-4,5-dimethyloxazole (**11b**) and 4,5-dimethyl-2-(4-(octyloxy)phenyl) oxazole (**11e**) were elucidated by SCXRD (Figure 5.14)**.** Crystals of both compounds were obtained from slow evaporation of diethyl ether solution at room temperature. A suitable crystal was selected and data were collected at 293 K using CuKα (λ = 1.5418 Å) radiation on an Xcalibur, Eos, Gemini diffractometer. Both structures were solved and refined using Olex2 [41]. The structure was solved with the Superflip [42] structure solution program using Charge Flipping and refined with the ShelXL [43] refinement package using Least Squares minimization.

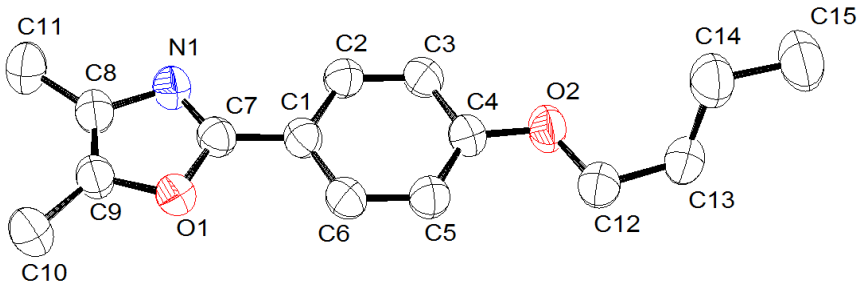

2-(4-Butyloxyphenyl)-4,5-dimethyloxazole (**11b**)

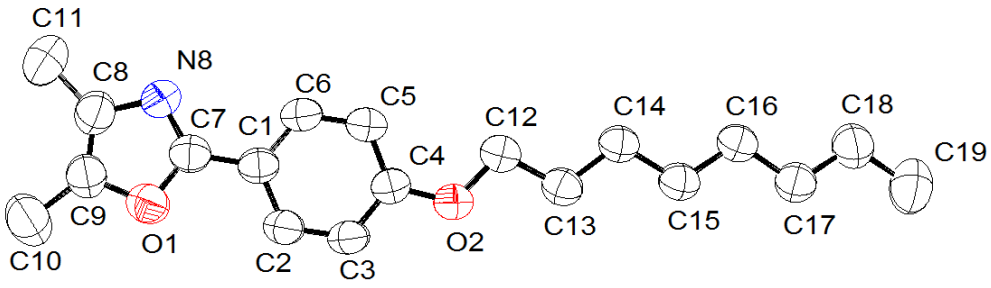

2-(4-(Octyloxy)phenyl)-4,5-dimethyloxazole (**11e**)

Figure 5.14 Molecular structure of 2-(4-butyloxyphenyl)-4,5-dimethyloxazole (**11b**) and 2-(4-(octyloxy)phenyl)-4,5-dimethyloxazole (**11e**). Ellipsoids are drawn at the 50% probability level and H atoms have been omitted for clarity

The compound **11b** crystallizes in monoclinic system with space group P21/c. The oxazole ring was almost planar to the benzene ring (Table 5.1). Compound **11e** crystallizes in triclinic system with space group *P-1*. Similar to compound **11b**, both benzene ring and oxazole ring were almost co-planar to each other.

Table 5.1 Values of torsion angles and length of short contacts of compound **11b** and **11e**

Compounds	**Torsion angles**		**Length of short contacts**	
11b	O1C7C1C6	(4.33^{o})	O1-H11	2.65 Å
	N1C7C1C2	(2.07^{o})	C4-H12a	2.89 Å
11e	O1C7C1C6	(2.07^{o})	O2-H3	2.65 Å
	N8C7C1C2	(2.09^{o})	N8-H10b	2.55 Å

Interestingly, the incorporation of *o*-butyl substituent on the ethereal linkage changes the structural and electronic features of the molecule that apparently modify the number and nature of non-covalent interactions. For instance, the C12-H12a group associated with the methylene moiety which is indeed in a close proximity to the ethereal linkage and the centroid of the benzene ring (Cg), essentially involved in the intermolecular C-H…π , (distance 2.89 Å) donor-acceptor interactions, arranging the molecules linearly along c-axis as shown in the following Figure 5.15. Whereas, C-H group of one of the methyl of oxazole is mainly involved in C-H…O (distance 2.65 Å) weak hydrogen bonding interactions, arranging the molecules along *b*-axis in *zig-zag* networking (Figure 5.16).

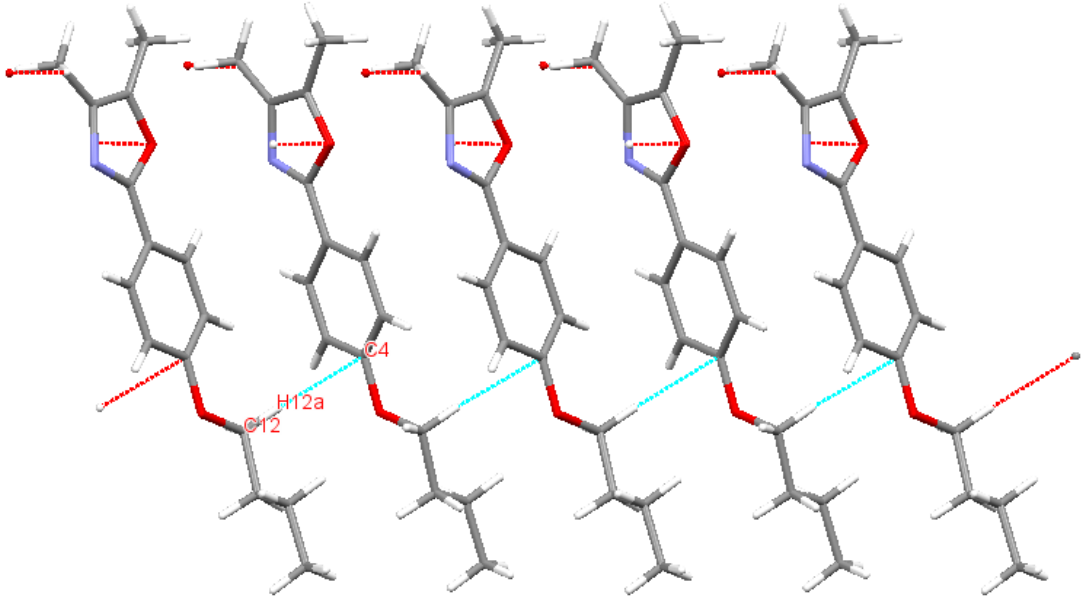

Figure 5.15 Arrangement of molecules through C-H…π intermolecular contacts along *c*-axis

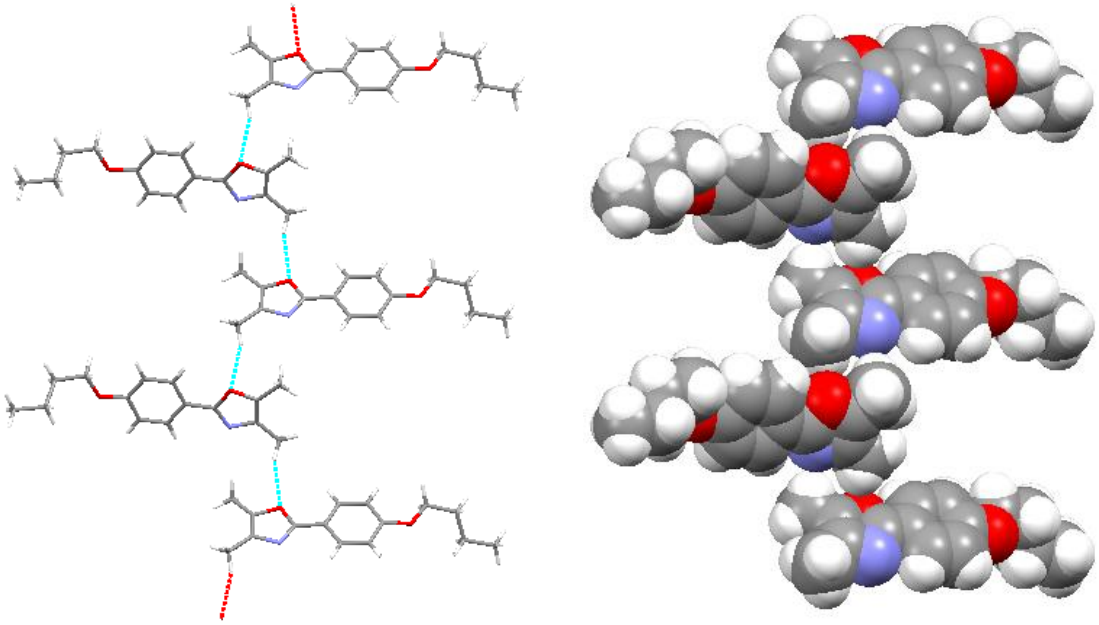

(a) (b)

Figure 5.16 Arrangement of molecules through C-H…O weak H-bonding intermolecular interactions along *b*-axis forming a *zig-zag* networking (a) capped Sticks and (b) spacefill representation of molecular packing

Interestingly, molecules of compound **11e** showed a number of intermolecular C-H…O and C-H…N interactions (Figure 5.17). For instance, the molecule present in the asymmetric unit forms a close contact with neighbouring molecules, arranging the neighbouring molecule in an anti-parallel fashion through C-H…O interactions involving C3-H3 group of benzene and ethereal oxygen atoms (Table 5.1). Principally, the oxazole moiety of the asymmetric molecule is involved in C-H…N donor-acceptor interaction, arranging the neighbouring molecule parallel along *a*-axis as shown in Figure 5.17. Overall, the asymmetric molecule forms an aggregate of three molecules. In fact, C10-H10b and N8 groups of oxazole moiety are mainly involved C-H…N (distance 2.55 Å) weak H-bonding interactions and arranging the molecules linearly along *a*-axis as shown in Figure 5.17.

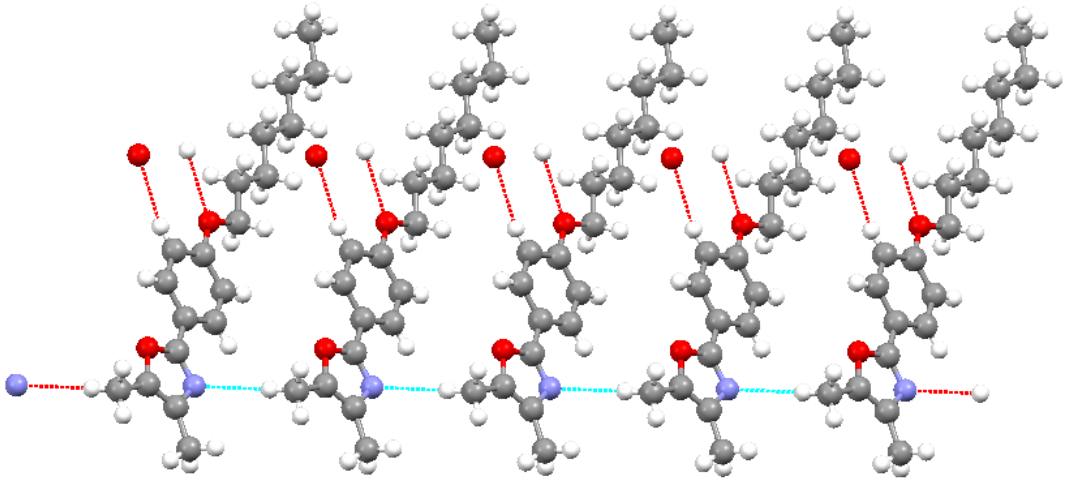

Figure 5.17 A linear arrangement of molecules of compound **11e** involving C-H…N interactions forming 1D chain-like structure

5.7.3 Computational Data.

DFT calculations were performed using Gaussian 09 program [31] with B3LYP functional and 6-311G(++) basis set on the series of the reported compounds.

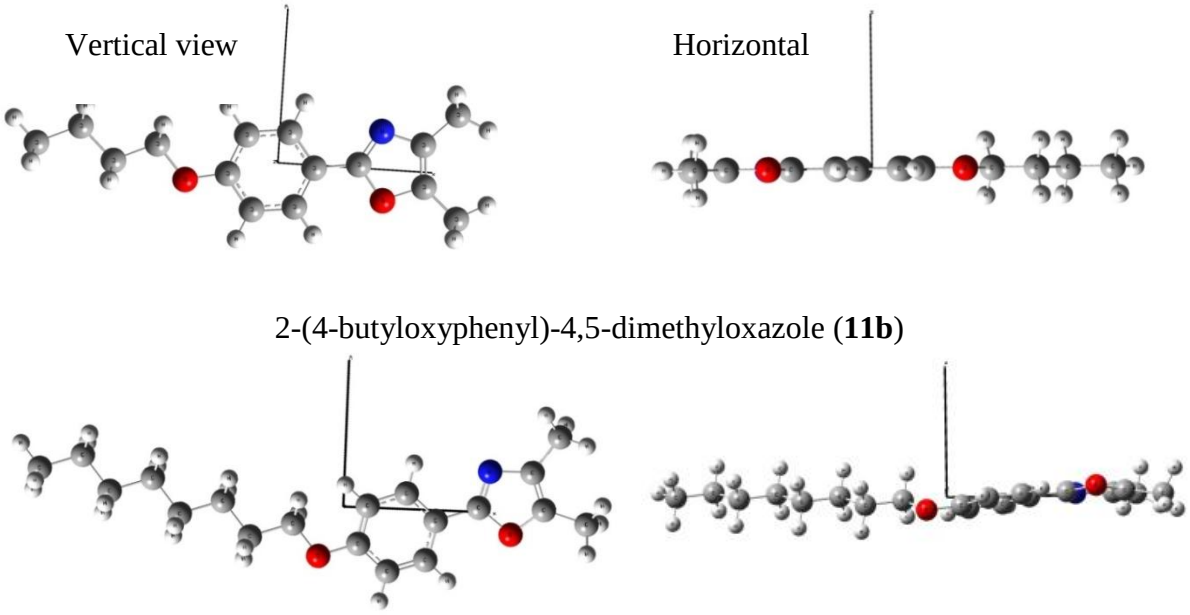

Figure 5.18 Optimized structure of compound **11b** and **11e** (Vertical and Horizontal view)

It was observed that geometric parameters of the optimized structures are in good agreement with that from the SCXRD data. The optimized structures of all oxazole derivatives showed co-planarity between phenyl and oxazole rings (**11e** dihedral angles for O1C7C1C6 and N1C7C1C2 was 0.47^{o} and 0.6^{o} respectively) which is in congruence with SCXRD data (Figure 5.18) (Table 5.2).

Table 5.2 Optimized structures of compound **11a**, **11c**, **11d**, **13b** and **15**

	Vertical view	**Horizontal view**
11a	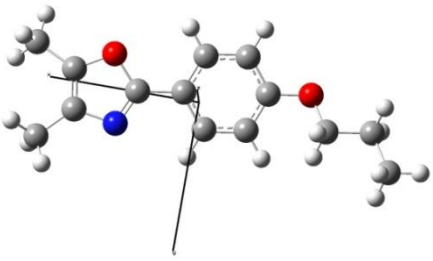	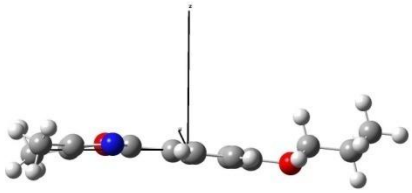
11c	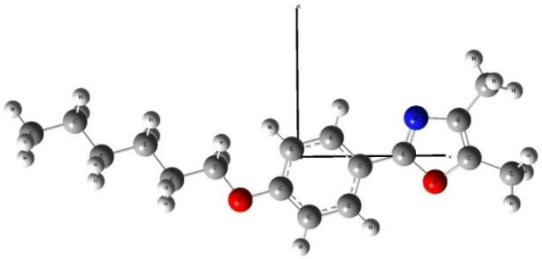	
11d	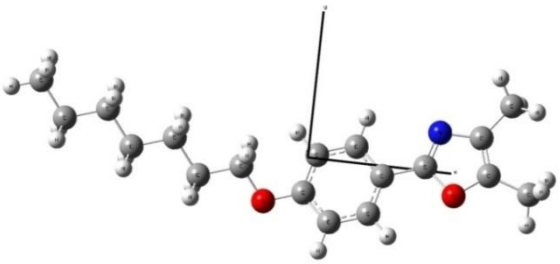	
13b	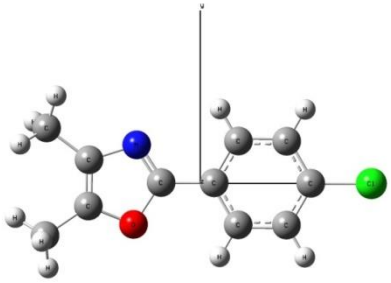	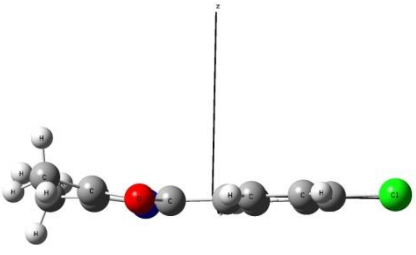

15

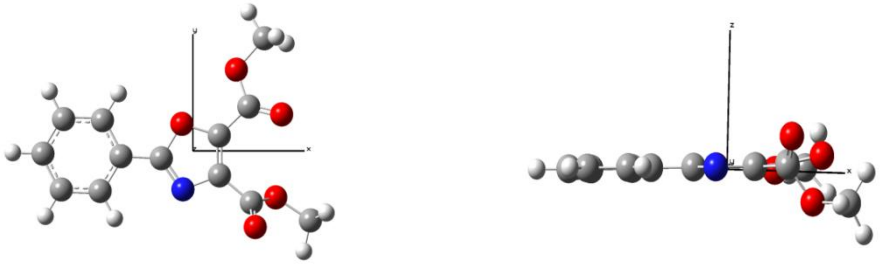

Calculated IR spectra of these series of compounds were compared with the experimental spectra. We presented intense vibrational modes in frequency region from 400 to 4000 cm^{-1}. It was concluded that in compound **11e**, band 847 cm^{-1} which corresponds to 867 cm^{-1} of calculated one was arises due to C-H out of plane deformation of phenyl ring. The 1019 cm^{-1} band observed was from C-O stretching (1021 cm^{-1} calculated). The calculated frequency 1213 cm^{-1} occurred from C-H in plane deformation of phenyl ring which was experimentally found at 1256 cm^{-1}. C-C Skeletal vibrations of phenyl ring found at 1472 cm^{-1} and 1649 cm^{-1} which was confirmed by 1453 cm^{-1} and 1648 cm^{-1} (calculated). Asymmetric CH_3 stretching was observed 2989 cm^{-1}corresponds to the calculated 2991 cm^{-1}. For compounds **11a**, **11b**, **11c** and **11d** similar data was obtained.

In compound **13b**, C-Cl stretching (calculated 770 cm^{-1}) observed at 790 cm^{-1} while C-H out of plane deformation of phenyl ring (calculated 874 cm^{-1}), C-C skeletal vibrations of phenyl ring (calculated 1517 cm^{-1})and asymmetric CH_3 stretching (calculated 3016 cm^{-1}) were found at 856 cm^{-1}, 1502 cm^{-1} and 3021 cm^{-1}, respectively. In compound **15**, 1737 cm^{-1} and 1689 cm^{-1} band corresponds to C=O stretching of ester group which were obtained at 1653 cm^{-1} and 1697 cm^{-1} in theoretical one.

Table 5.3. IR spectra values obtained from experimental and DFT calculations

Compound	Experimental (cm^{-1})	DFT Calculations (cm^{-1})
11e	2989, 1649, 1615, 1560, 1503, 1472, 1344, 1307, 1256, 1172, 1019, 847.	3013, 2992, 1673, 1648, 1522, 1453, 1254, 1213,1021, 988, 867
13b	3021, 2950, 1611, 1502, 1450, 856 790	3109, 3067, 3016, 1668, 1517, 1437, 1093, 1040, 874, 770
15	3035, 2957, 1737, 1689, 1608, 1508, 1473, 1435, 1259, 1042, 992, 914, 799, 768, 699, 549	3188, 3049, 1697, 1653, 1516, 1377, 1287, 1081, 807.

5.8 Conclusion

A series of 2,4,5-trisubstituted oxazole were prepared and characterized by standard spectroscopic methods and X-ray crystallography. The crystal structures of compound **13b** and compound **13e** shows significant nonbonding intermolecular interactions such as C-H...π, C-H...N and C-H...O interactions, forming a fascinating 1D and 3D molecular networking, respectively.

5.9 Experimental

5.9.1 General

All the chemicals were reagent grade and used as purchased. Moisture-sensitive reactions were performed under an inert atmosphere of dry nitrogen with dried solvents. Reactions were monitored by TLC analysis using Merck 60 F254 aluminium coated plates and the spots were visualized under UV light. Column chromatography was carried out on Silica gel (60-140 mesh). All melting points were determined using Thiele's tube using paraffin oil and are uncorrected. IR spectra were recorded in range from 4000-400 cms^{-1} using KBr pellets on a Shimadzu Prestige 21 spectrometer with 4 scan numbers. NMR spectra were recorded on a Bruker Avance-III 400 spectrometer in $CDCl_3$. Diffraction data were collected using CuKα (λ = 1.5418 Å) radiation on an Xcalibur, Eos, Gemini diffractometer.DFT calculations were performed using Gaussian 09 program with B3LYP functional and 6-311G(++) basis set.

5.9.2 Synthesis

4-Alkyloxybenzamide was synthesized from 4-hydroxy benzoic acid in three steps by following the reported procedure [44].

A mixture of 3-chloro-2-butanone (1.17 g, 0.014 mol) and 4-alkyloxy benzamide (**10a-e**) (0.028 mol) in glacial acetic acid (1.5 mL) was stirred at 120 ^{o}C under nitrogen atmosphere for 18 hours. The reaction mixture was cooled to room temperature. The reaction mixture was neutralized by adding saturated solution of K_2CO_3 (10 mL). The neutralized reaction mixture was extracted with dichloromethane (3 x 10 mL). The organic phase was separated, dried over anhydrous sodium sulphate and concentrated under reduced pressure. The crude product was purified by column chromatography on silica gel with ethyl acetate and petroleum ether (1:20) to afford compound **11a-e**.

5.9.2.1 4,5-Dimethyl-2-(4-propoxyphenyl)oxazole (11a)

Yield: 38%. M.p. 59-61^{o}C. ^{1}H NMR (400 MHz, $CDCl_3$): δ 1.059 (t, 3H), 1.811-1.863 (q, 2H), 2.152 (s, 3H), 2.304 (s, 3H), 3.968 (t, 2H), 6.931-6.960 (d, 2H, ArH), 7.900-7.933 (d, 2H, ArH). ^{13}C NMR (100 MHz, $CDCl_3$): δ (ppm) 10.04, 10.50, 11.27, 22.53, 69.52, 114.53, 120.46, 127.38, 131.42, 142.62, 159.27, 160.42. IR (KBr, cm^{-1}): ν 854, 1170, 1250, 1414, 1500, 1550, 1650, 2990.

5.9.2.2 2-(4-Butoxyphenyl)-4,5-dimethyloxazole (11b)

Yield: 40%. M.p. 60-62 ^{o}C. ^{1}H NMR (400 MHz, $CDCl_3$): δ 0.997-0.983 (t, 3H, -CH_3), 1.508-1.523 (m, 2H, -CH_2), 1.781-1795 (m, 2H, -CH_2), 2.144 (s, 3H, -CH_3), 2.29 (s, 3H, -CH_3), 3.998-4.009 (t, 2H, -OCH_2), 6.933 (d, 2H, ArH), 7.902 (d, 2H, ArH). ^{13}C NMR (100 MHz, $CDCl_3$): δ (ppm) 10.07, 11.29, 13.86, 19.23, 31.26, 67.76, 114.55, 120.47, 127.40, 131.44, 142.64, 159.29, 160.45. IR (KBr, cm^{-1}): ν 844, 1151, 1174, 1248, 1384, 1423, 1499, 1532, 1550, 1584, 1630, 1640, 2981.

5.9.2.3 2-(4-(Hexyloxy)phenyl)-4,5-dimethyloxazole (11c)

Yield: 35%. M.p. 74-75 ^{o}C. ^{1}H NMR (400 MHz, $CDCl_3$): δ 0.921-0.938 (t, 3H, -CH_3), 1.333-1.368 (m, 4H,-CH_2), 1.457-1.493 (m, 2H, -CH_2), 1.784-1.820 (m, 2H, -CH_2), 2.149 (s, 3H, -CH_3), 2.302 (s, 3H, -CH_3), 3.977-4.014 (t, 2H, -OCH_2), 6.926-6.948 (d, 2H, ArH), 7.897-7.897 (d, 2H, ArH). ^{13}C NMR (100 MHz, $CDCl_3$): δ (ppm): 10.07, 11.29, 14.05, 22.61, 25.71, 29.17, 31.59, 68.06, 114.53, 120.45, 127.38, 131.43, 142.62, 159.28, 160.43. IR (KBr, cm^{-1}): ν 740, 842, 1028, 1179, 1248, 1309, 1422, 1474, 1500, 1559, 1612, 1648, 2976.

5.9.2.4 2-(4-(Heptyloxy)phenyl)-4,5-dimethyloxazole (11d)

Yield: 35%. M.p. 77-79 ^{o}C. ^{1}H NMR (400 MHz, $CDCI_3$): δ 0.911 (t, 3H), 1.300-1.341 (m, 6H), 1.356-1.498 (m, 2H), 1.772-1.843 (m, 2H), 2.306 (s, 3H), 2.308 (s, 3H), 4.00 (t, 2H), 6.928-6.957 (d, 2H, ArH), 7.899-7.922 (d, 2H, ArH). ^{13}C NMR (100 MHz, $CDCl_3$): δ (ppm): 10.08, 11.30, 14.10, 22.62, 25.99, 29.07, 29.22, 31.78, 68.09, 114.20, 114.55, 120.47, 127.39, 131.45, 142.63, 159.29, 160.44. IR (KBr, cm^{-1}): ν 850, 1022, 1170, 1250, 1415, 1505, 1560, 1600, 1650, 2995.

5.9.2.5 2-(4-(Octyloxy)phenyl)-4,5-dimethyloxazole (11e)

Yield: 37%. M.p. 78-79 ^{o}C. ^{1}H NMR (400 MHz, $CDCl_3$): δ 0.990-0.997 (t, 3H, -CH_3), 1.329-1.372 (m, 8H, -CH_2), 1.432-1.494 (m, 2H, -CH_2), 1.789-1.843 (m, 2H, -CH_2), 2.154 (s, 3H, -CH_3), 2.308 (s, 3H, -CH_3), 3.987-4.020 (t, 2H, -OCH_2), 6.930-6.952 (d, 2H, ArH), 7.899-7.921 (d, 2H, ArH). ^{13}C NMR (100 MHz, $CDCl_3$): δ (ppm): 10.10, 11.31, 14.13, 22.68, 26.03, 29.22, 29.25, 29.36, 31.82, 68.09, 114.55, 120.47, 127.40, 131.44, 142.64, 159.30, 160.44. IR (KBr, cm^{-1}): ν 2989, 1649, 1615, 1560, 1503, 1472, 1344, 1307, 1256, 1172, 1019, 847.

5.9.2.6 General procedure for the synthesis of 4,5-dimethyl-2-phenyloxazole (13a) and 2-(4-chlorophenyl)-4,5-dimethyloxazole (13b)

A mixture of 3-chloro-2-butanone (1.17 g, 0.014 mol) and benzamide (**12a** and **12b**) (0.028 mol) in glacial acetic acid (1.5 mL) was stirred at 120 ^{o}C under nitrogen atmosphere for 18 hours. The reaction mixture was cooled to room temperature. The reaction mixture was neutralized by adding saturated solution of K_2CO_3 (10 mL). The neutralized reaction mixture was extracted with dichloromethane (3 x 10 mL). The organic phase was separated, dried over anhydrous sodium sulphate and concentrated under reduced pressure. The crude product was purified by column chromatography on silica gel with ethyl acetate and petroleum ether (1:20) to afford compound **13**.

5.9.2.7 4,5-Dimethyl-2-phenyloxazole (13a)

Yield: 44%. M.p. 49-50 ^{o}C (lit., 50-52 ^{o}C) [25].^{1}H NMR (400 MHz, $CDCI_3$): δ 2.2 (s, 3H), 2.4 (s, 3H), 7.43-7.45 (m, 3H, ArH), 7.98-8.03 (m, 2H, ArH).

5.9.2.8 2-(4-Chlorophenyl)-4,5-dimethyloxazole (13b)

Yield: 52%. M.p. 121-123 ^{o}C (lit., 122-124 ^{o}C).[26] ^{1}H NMR (400 MHz, $CDCI_3$): δ 2.168 (s, 3H), 2.326 (s, 3H), 7.400-7.428 (m, 2H, ArH), 7.911-7.933 (m, 2H, ArH). ^{13}C NMR (100 MHz, $CDCl_3$): δ (ppm): 10.12, 11.28, 126.31, 127.08, 132.13, 135.64, 143.74, 158.21. IR (KBr, cm^{-1}): ν 3021, 2950, 1611, 1502, 1450, 856, 790.

5.9.2.9 Synthesis of dimethyl 2-phenyloxazole-4,5-dicarboxylate (15)

To the stirred slurry of N-benzoyl glycine 2.0 g in 30 mL of dry THF, 14.2 g (10 equivalents) of oxalyl dichloride was added dropwise under N_2 atmosphere. After complete addition, mixture was stirred for overnight. The excess of oxalyl dichloride was removed and reaction mixture was concentrated under low pressure. To this mixture 1.7 mL (1.5 equivalents) of triethyl amine and 15 mL of dry MeOH was added. This solution was stirred for 3 hours at room temp. The residue was concentrated under reduced pressure and crude product was purified by column chromatography (petroleum ether: ethyl acetate) to yield 2.4 g as a white solid compound.

Yield: 20%, M.p. 47-48 ^{o}C (lit., 45-47^{o}C) [34]. ^{1}H NMR (400 MHz, $CDCl_3$): δ 3.949 (s, 3H), 4.037 (s, 3H), 7.551-7.559 (t, 2H), 7.613-7.653 (t, 1H), 7.930-7.954 (d, 2H). ^{13}C NMR (100 MHz, $CDCl_3$): δ (ppm): 53.54, 127.84, 129.09, 131.35, 133.37, 142.03, 162.62, 163.45, 166.46. IR (KBr, cm^{-1}): ν 3035, 2957, 1737, 1689, 1608, 1508, 1473, 1435, 1259, 1042, 992, 914, 799, 768, 699, 549.

5.10 Spectra

5.10.1 4, 5-Dimethyl-2-(4-propoxyphenyl)oxazole (11a)

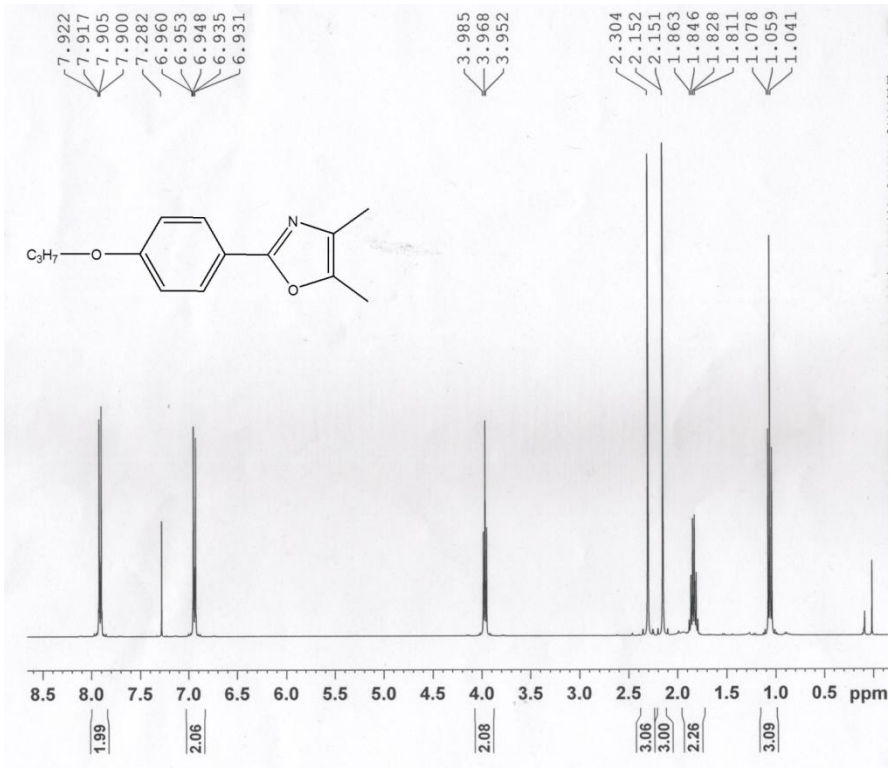

^{1}H NMR spectrum

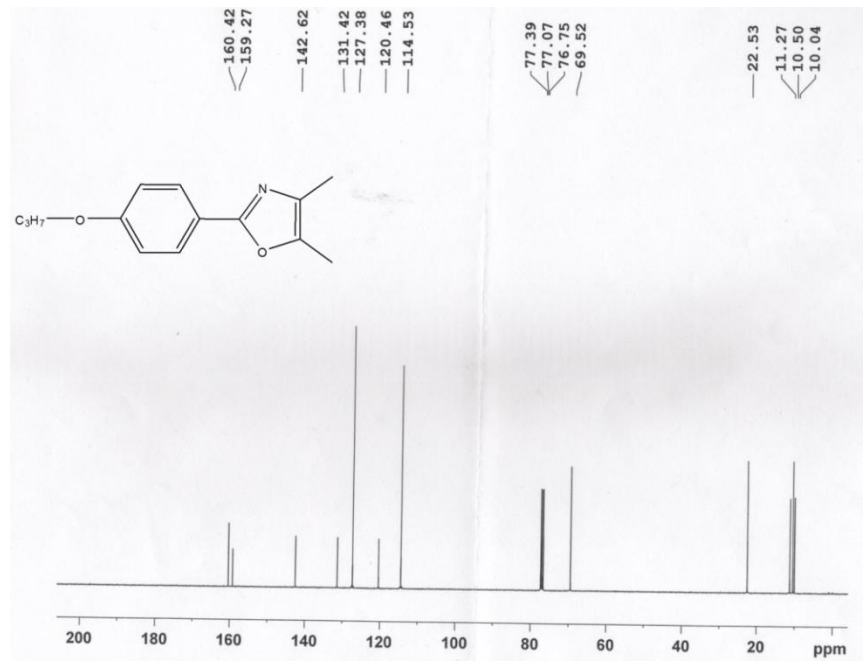

^{13}C NMR spectrum

5.10.2 4, 5-Dimethyl-2-(4-butyloxyphenyl)oxazole (11b)

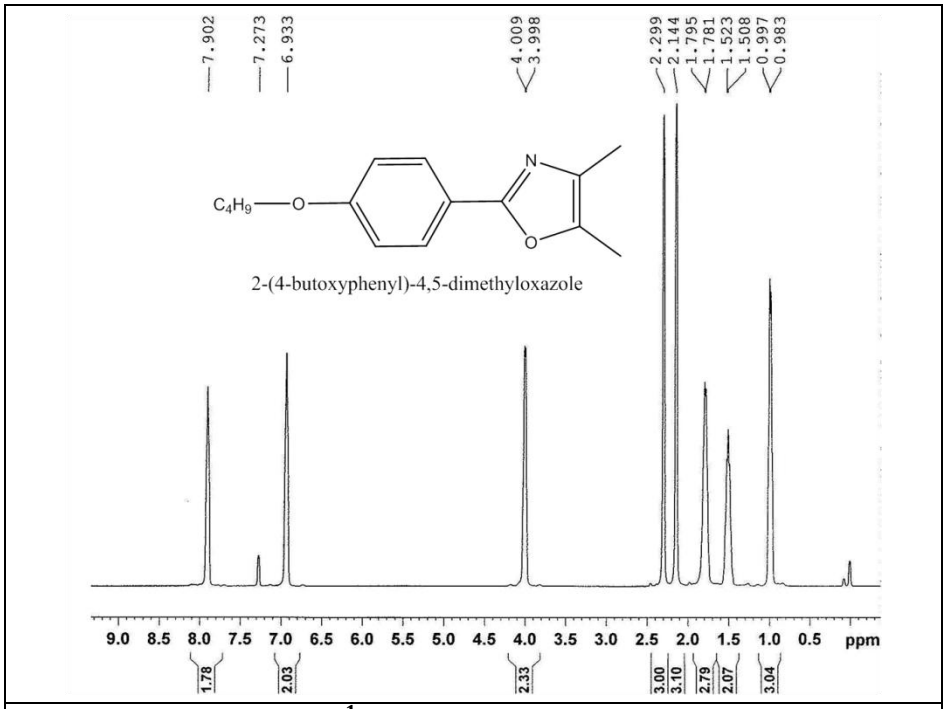

^{1}H NMR spectrum

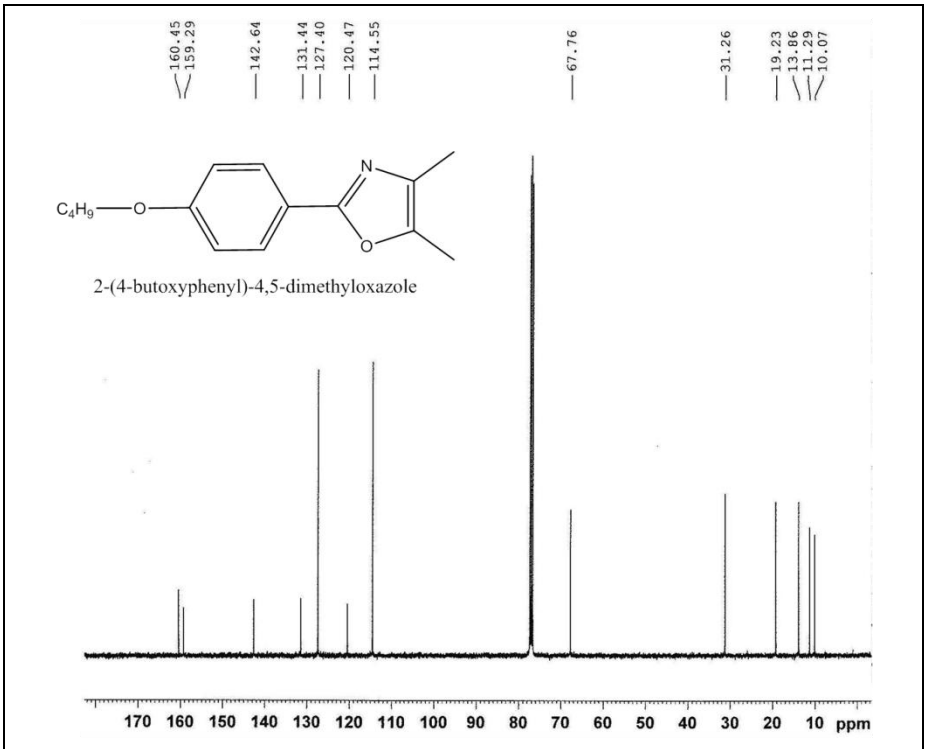

^{13}C NMR spectrum

5.10.3 4, 5-Dimethyl-2-(4-hexyloxyphenyl)oxazole (11c)

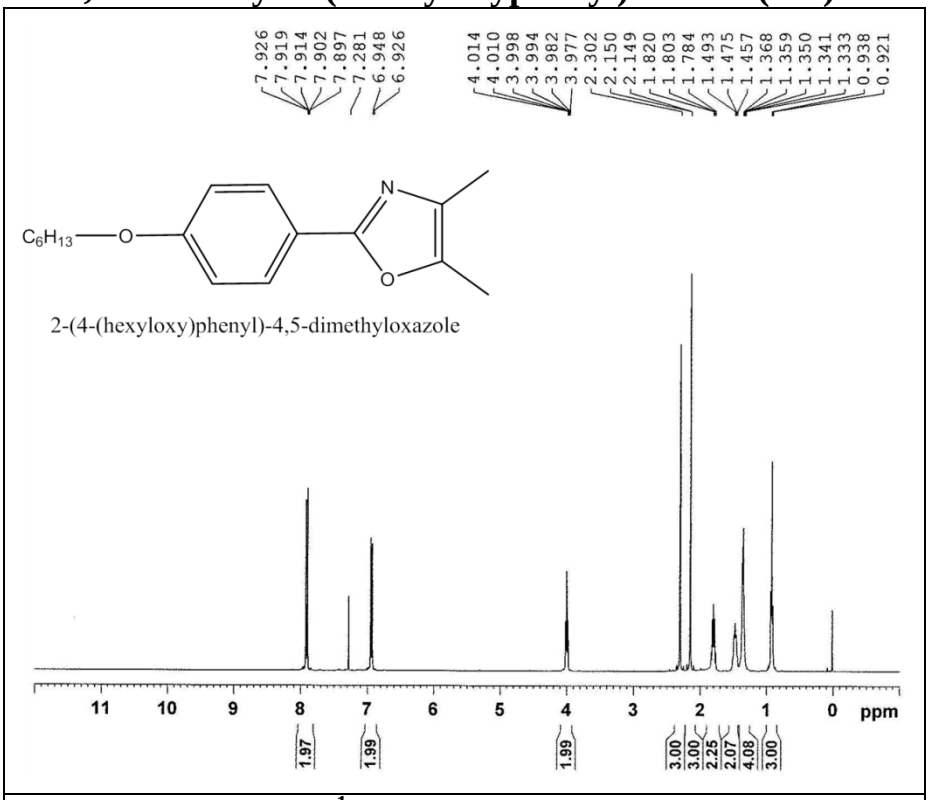

^{1}H NMR spectrum

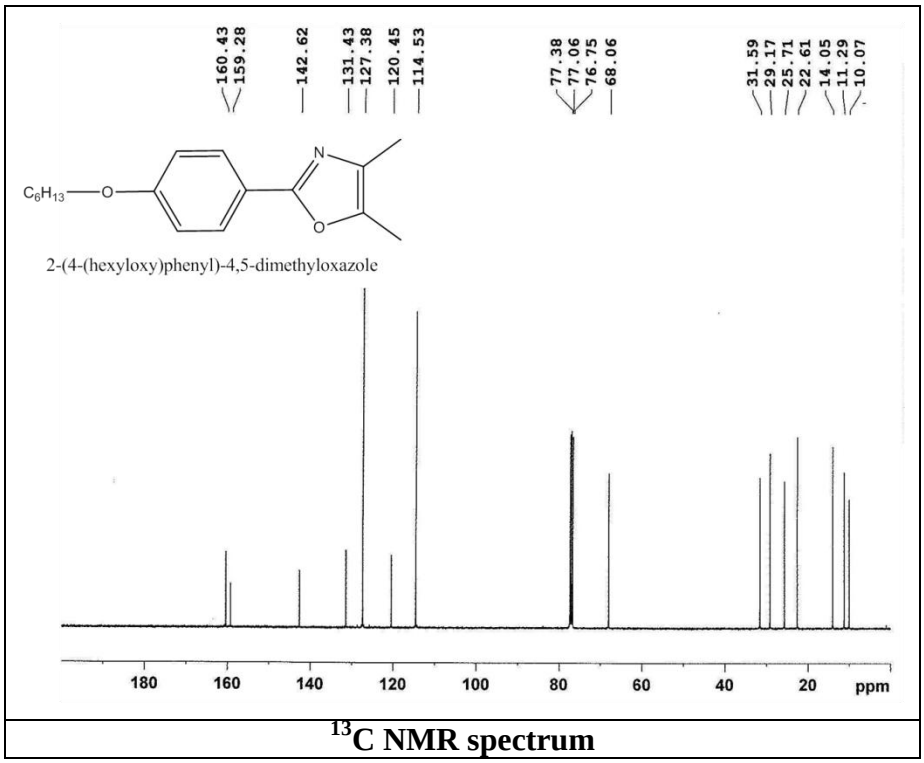

^{13}C NMR spectrum

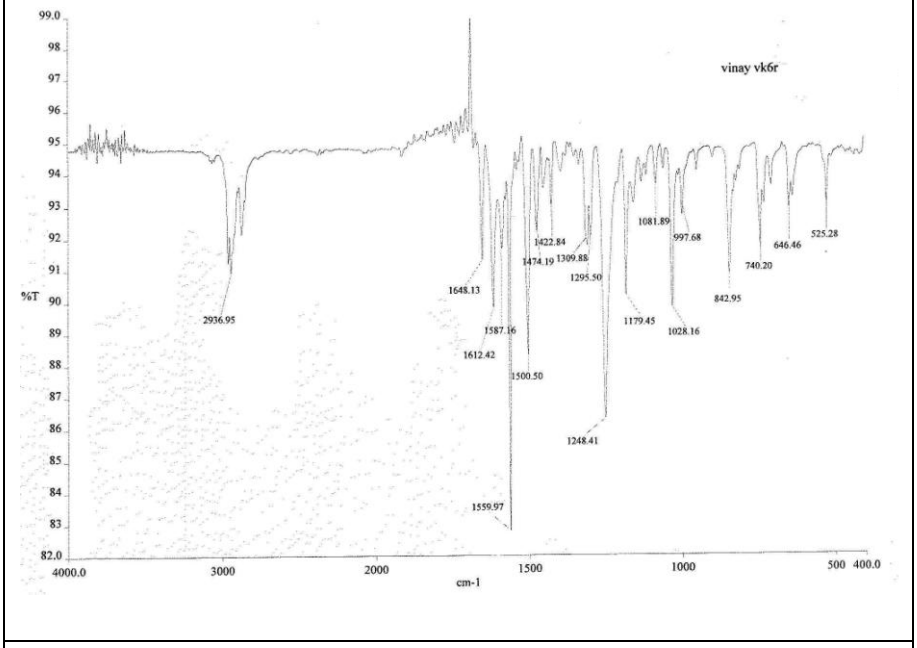

IR spectrum

5.10.4 4, 5-Dimethyl-2-(4-heptyloxyphenyl)oxazole (11d)

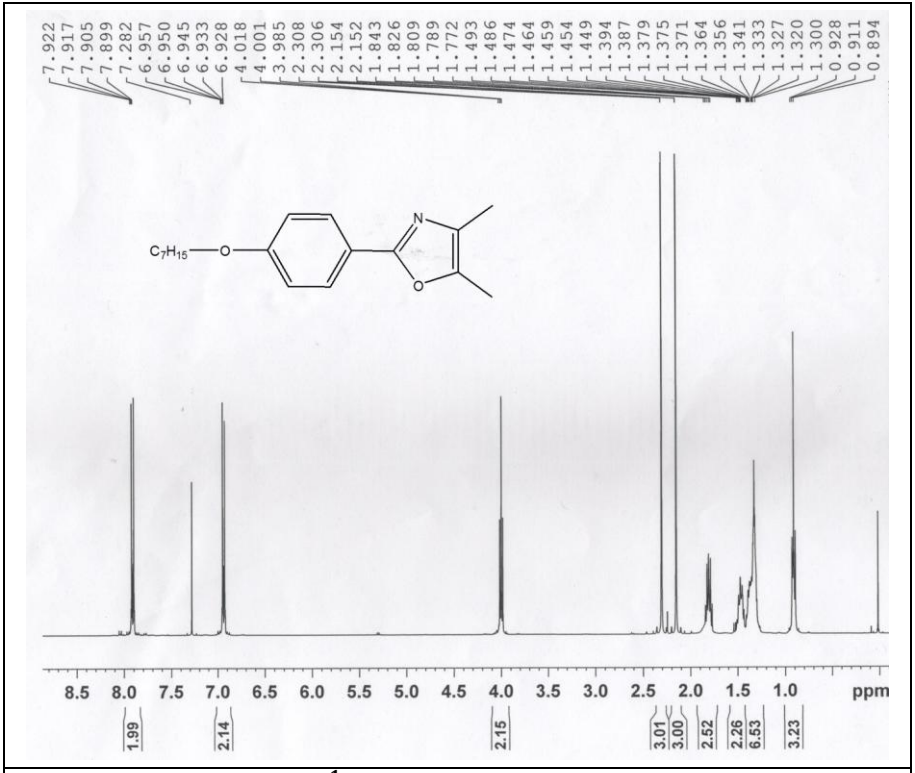

^{1}H NMR spectrum

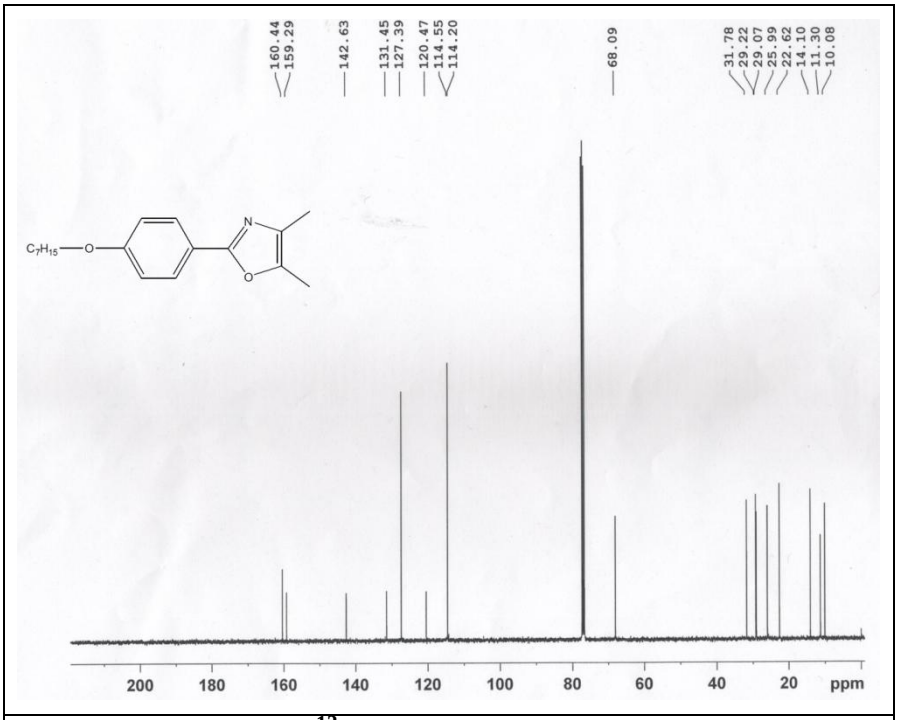

^{13}C NMR spectrum

5.10.5 4, 5-Dimethyl-2-(4-octyloxyphenyl)oxazole (11e)

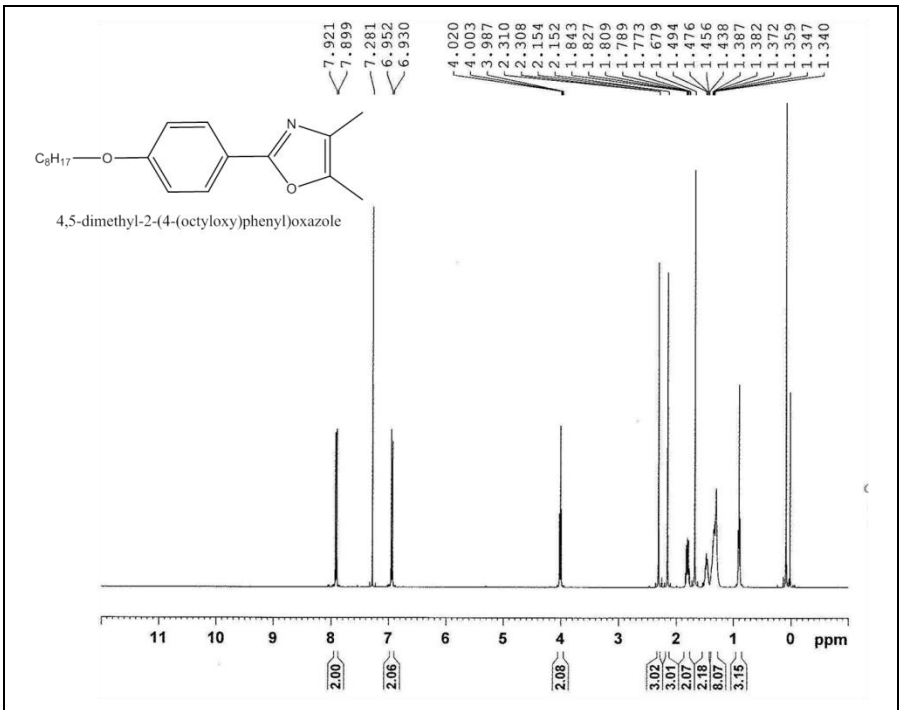

^{1}H NMR spectrum

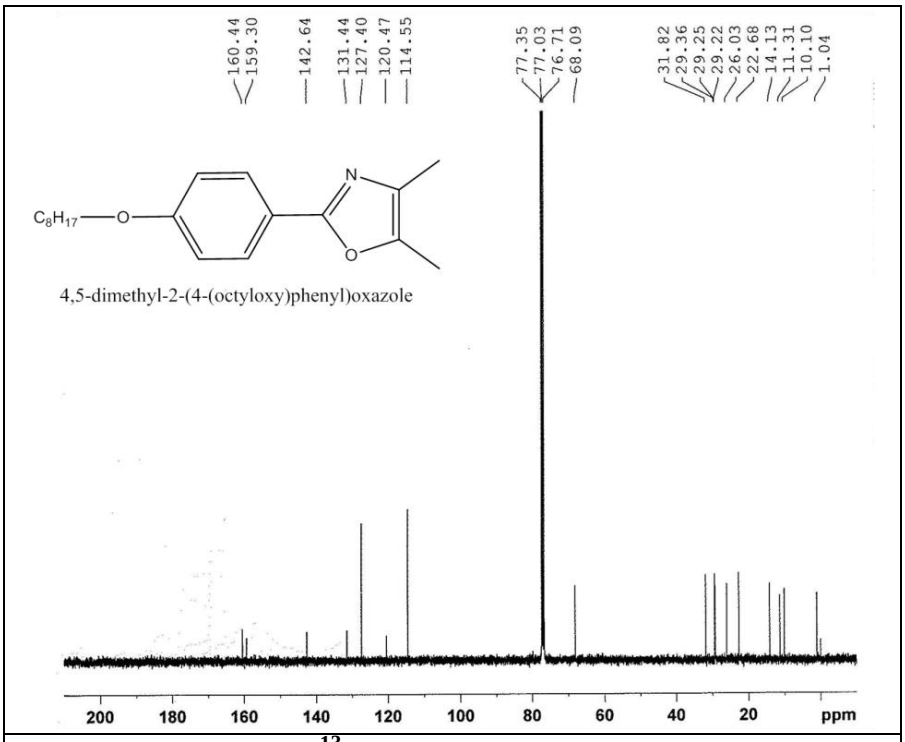

^{13}C NMR spectrum

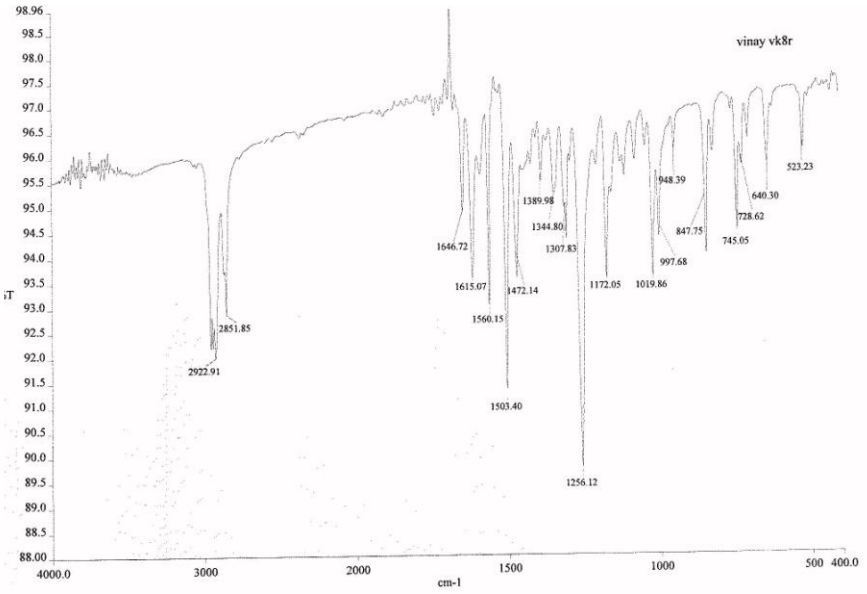

IR spectrum

5.10.6 4, 5-Dimethyl-2-phenyloxazole (13a)

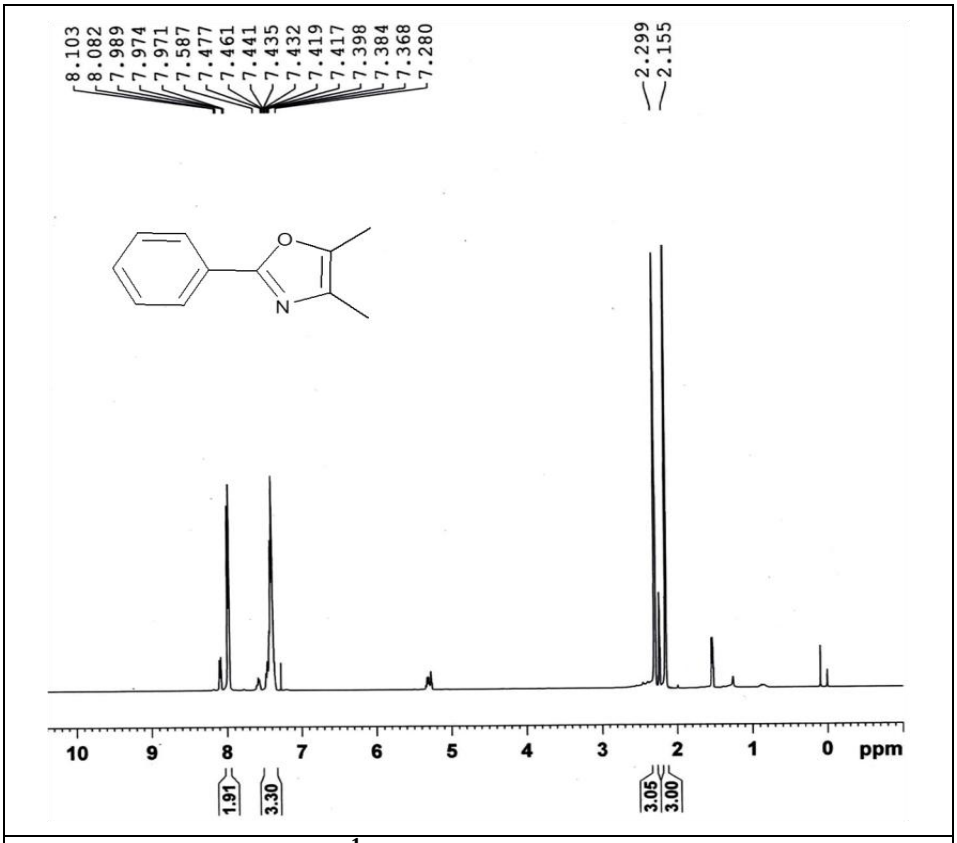

^{1}H NMR spectrum

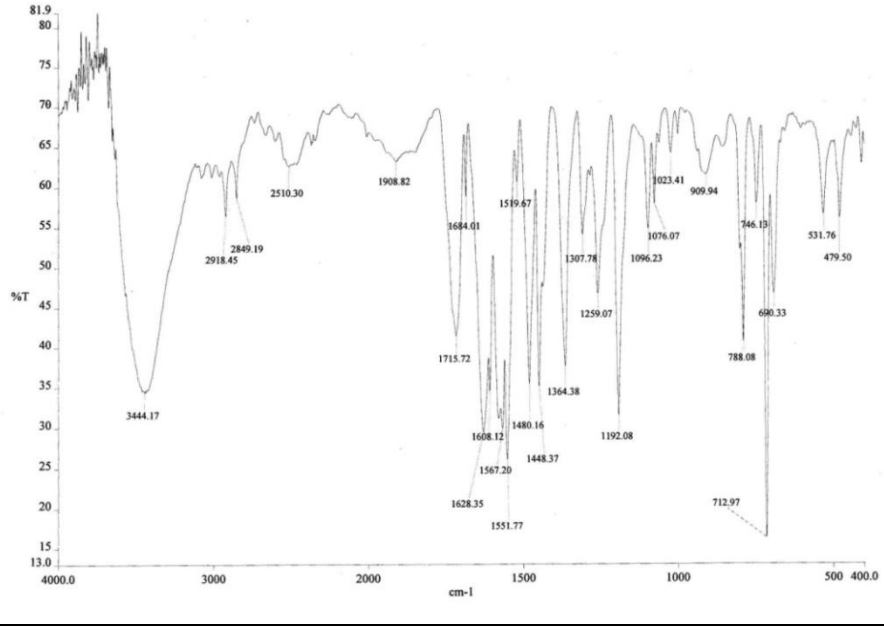

IR spectrum

5.10.7 2-(4-Chlorophenyl)-4, 5-dimethyloxazole (13b)

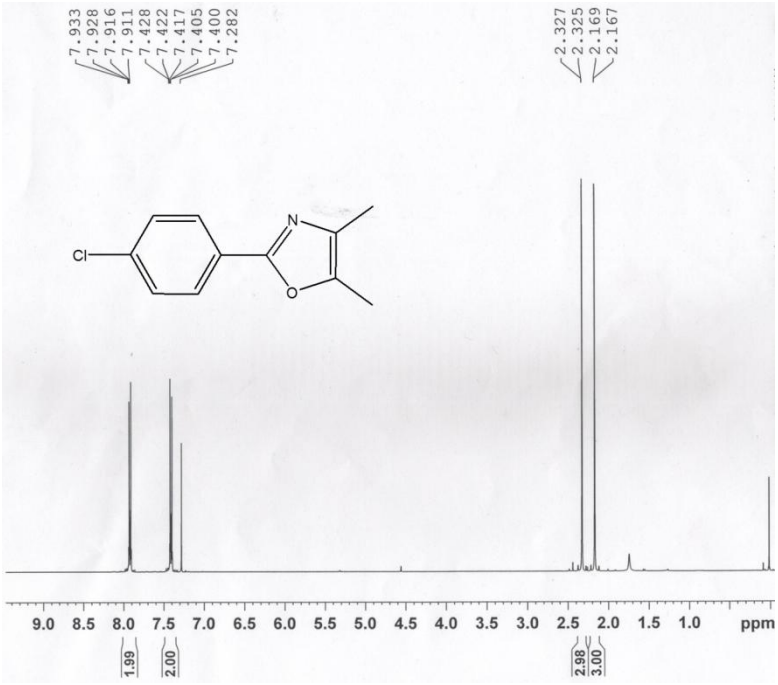

^{1}H NMR spectrum

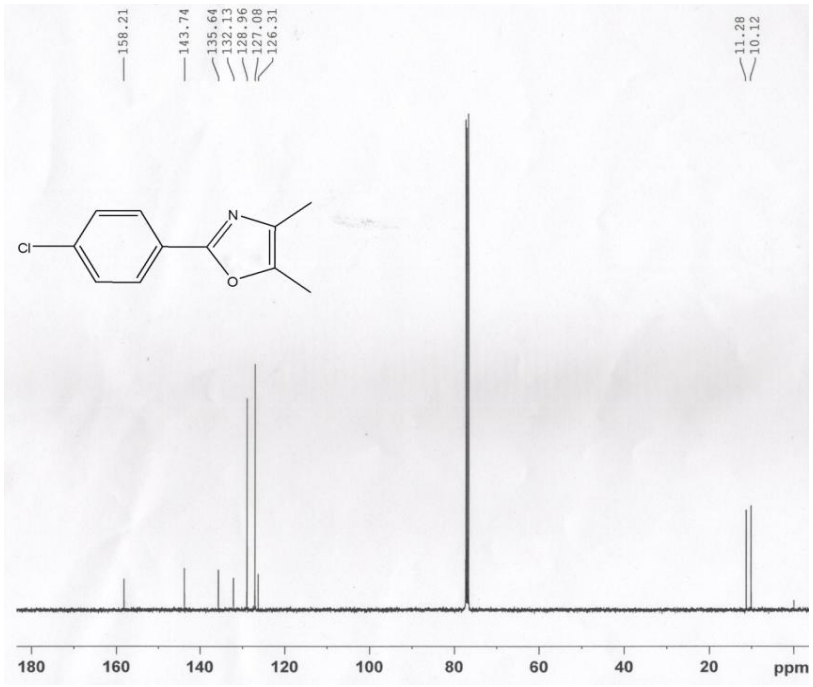

^{13}C NMR spectrum

5.10.8 Dimethyl 2-phenyloxazole-4, 5-dicarboxylate (15)

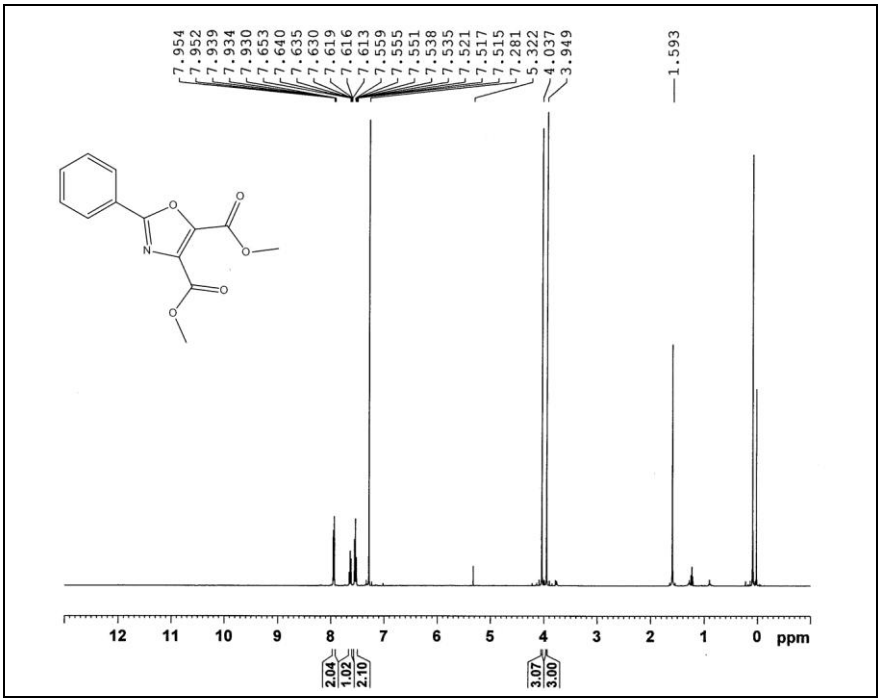

^{1}H NMR spectrum

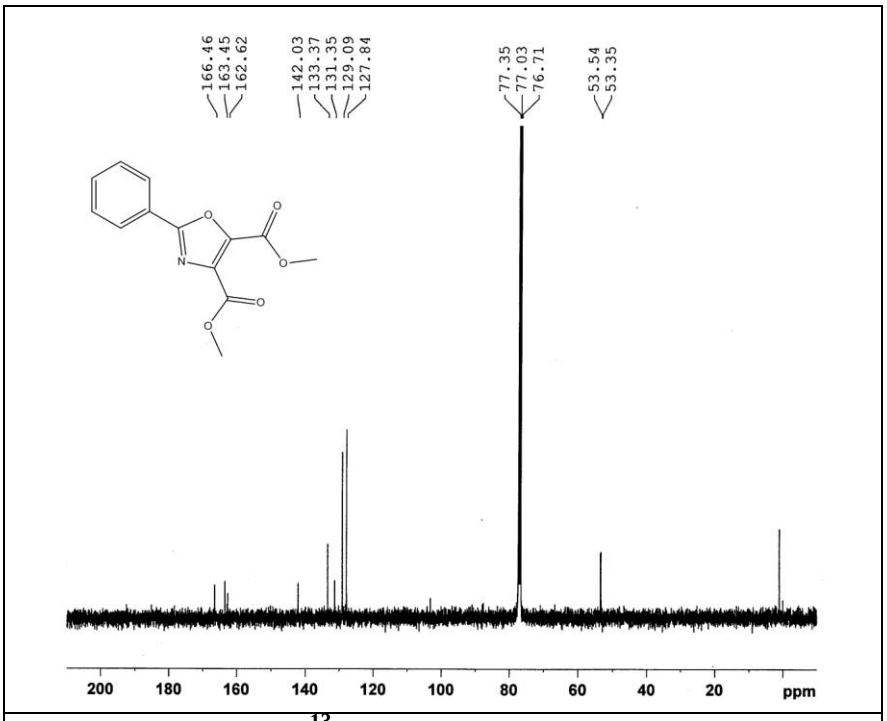

^{13}C NMR spectrum

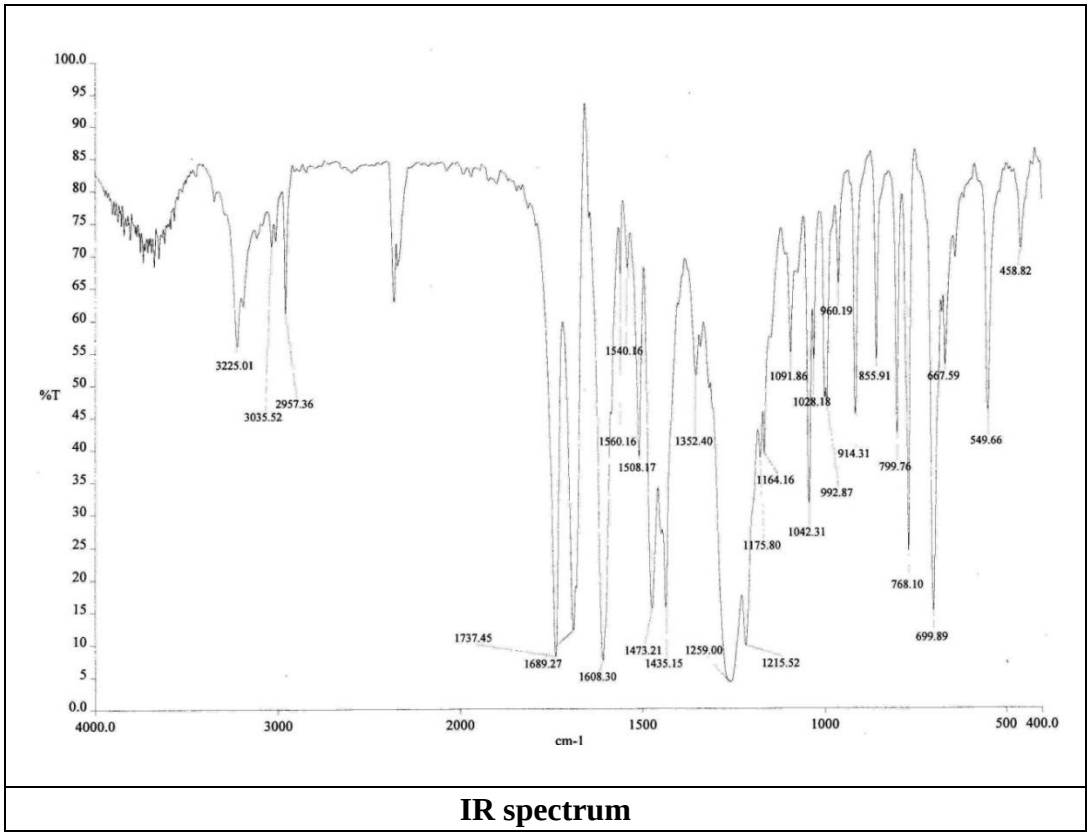

IR spectrum

5.10.9 Crystal data and structure refinement for Compound 11b and Compound 11e

Compound	11b	11e
Empirical formula	$C_{15}H_{19}NO_2$	$C_{19}H_{27}NO_2$
Formula weight	245.31	301.43
Crystal system	monoclinic	Triclinic
Temperature /K	293(2)	298
Space group	P21/c	P-1
a/Å	15.1739(5)	6.2142(5)
b/Å	10.9792(3)	7.8709(6)
c/Å	8.28616(19)	20.0780(15)
α/°	90.00	92.439(6)
β/°	96.222(3)	95.360(6)
γ/°	90.00	112.027(8)
Volume/$Å^3$	1372.31(6)	903.17(13)
Z	4	2
Pcalc mg/mm^3	1.187	1.1083
μ/mm^{-1}	0.624	0.555
F(000)	528.0	329.0
2Θ range for data collection	14.2 to 145.86°	12.18 to 143.54
Index ranges	$-18 \le h \le 18$, $-13 \le k \le 13$, $-10 \le l \le 7$	$-7 \le h \le 5$, $-6 \le k \le 9$, $-24 \le l \le 24$
Reflections collected	7983	5568
Independent reflections	2744 [R_{int} = 0.0241, R_{sigma} = 0.0224]	3446 [R_{int} = 0.0242, R_{sigma} = 0.0319]
Data/restraints/parameters	2723/0/166	3446/0/201
Goodness-of-fit on F2	1.059	1.077
Final R indexes [I>=2σ (I)]	R1 = 0.0486, wR2 = 0.1360	R_1 = 0.0668, wR_2 =0.1919
Final R indexes [all data]	R1 = 0.0528, wR2 = 0.1410	R_1 = 0.0802, wR_2 =0.2109
Largest diff. peak/hole /e $Å^{-3}$	0.18/-0.16	0.19/-0.20
CCDC no.	1030319	1032117

5.11 References

[1] (a) T. Figueira-Duarte and K. Mullen. *Chem. Rev*., 111, (2011), 7260. (b) Z. Hudson and S. Wang. *Acc. Chem. Res.*, 42, (2009), 1584.(c) Z. Chi, X. Zhang, B. Xu, X. Zhou, C. Ma, Y. Zhang, S. Liu and J. Xu. *Chem. Soc. Rev.*, 41, (2012), 3878.

[2] (a) T. Janosik, N. Wahlstrom, and J. Bergman. *Tetrahedron*., 64, (2008), 9159. (b) N. Hu, S. Xie, Z. Popovic, B. Ong and A. Hor, *J. Am. Chem. Soc*., 121, (1999), 5097. (c) H. Zhao, X. Tao, F. Wang, Y. Ren, X. Sun, J. Yang, Y. Yan, D. Zou, X. Zhao and M. Jiang. *Chem. Phys. Lett*., 439, (2007), 132. (d) H. Zhao, X. Tao, P. Wang, Y. Ren, J. Yang, Y. Yan, C. Yuan, H. Liu, D. Zou and M. Jiang. *Org. Electron*., 8, (2007), 673.

[3] H. Zhao, F. Wang, C. Yuan, X. Tao, J. Sun, D. Zou and M. Jiang. *Org. Electron*., 10, (2009), 925.

[4] P. Boudreault, S. Wakim, N. Blouin, M. Simard, C. Tessier, Y. Tao and M. Leclerc. *J. Am. Chem. Soc*., 129, (2007), 9125.

[5] J. Bergman, T. Janosik and N. Wahlstrom. *Adv. Heterocycl. Chem*., 80, (2001), 1.

[6] B. Robinson. *Chem. Soc*., 1963, 3097.

[7] H. Kim, C. Heo and H. Kim. *J. Am. Chem. Soc*., 135, (2013), 17969.

[8] J. Srivastava, D. Barber and M. Jacobson. *Physiology*., 22, (2007), 30.

[9] D. Lide, The Handbook of Chemistry and Physics, 89th ed CRC Press/Taylor & Francis Group: Boca Raton, FL. 2007. 2640

[10] P. Saluja, H. Sharma, N. Kaur, N. Singh and D. Jang. *Tetrahedron*., 68, (2012), 2289.

[11] N. Singh and D. Jang. *Org. let.*, 9, (2007), 1991.

[12] Y. Wu, J. You, K. Jiang, H. Wu, J. Xiong and Z. Wang. *Dyes Pigm.*, 149, (2018), 1.

[13] A. Kushwaha, S. Patil and D. Das. *New J. Chem*., 42, (2018), 9200.

[14] K. Aich, S. Das, S. Goswami, C. Quah, D. Sarkar, T. Mondal and H. Fun. *New J. Chem*., 40 (2016), 6907.

[15] (a) G. Chang, C. Chuang, J. Lee, Y. Chang, M. Leung and K. Hsieh. *Polymer.*, 54, (2013) 3548. (b) W. Lai, D. Liu and W. Huang. *Macromol. Chem. Phys.,* 212, (2011) 445. (c) S. Cai, G. Tian, X. Li, J. Su and H. Tian. J. *Mater. Chem. A.,* 1, (2013) 11295.

[16] L. Yudina and J. Bergman. *Tetrahedron.,* 59, (2003) 1265.

[17] V. Kadam, P. Bhatt, H. Karmakar, S. Zade and A. Patel. *ChemistrySelect.,* 4, (2019), 3948.

[18] J. Bredas, R. Silbey, D. Boudreaux and R. Chance. *J. Am. Chem. Soc*., 105, (1983), 6555.

[19] M. Frisch, G. Trucks, H. Schlegel, G. Scuseria, M. Robb, J. Cheeseman, G. Scalmani, V. Barone, B. Mennucci, G. Petersson, H. Nakatsuji, M. Caricato, X. Li, H. Hratchian, A. F. Izmaylov, J. Bloino, G. Zheng, J. L. Sonnenberg, M. Hada, M. Ehara, K. Toyota, R. Fukuda, J. Hasegawa, M. Ishida, T. Nakajima, Y. Honda, O. Kitao, H. Nakai, T. Vreven, J. A. Montgomery, Jr., J. Peralta, F. Ogliaro, M. Bearpark, J. Heyd, E. Brothers, K. Kudin, V. N. Staroverov, R. Kobayashi, J. Normand, K. Raghavachari, A. Rendell, J. Burant, S. Iyengar, J. Tomasi, M. Cossi, N. Rega, J. Millam, M. Klene, J. Knox, J. Cross, V. Bakken, C. Adamo, J. Jaramillo, R. Gomperts, R. Stratmann, O. Yazyev, A. J. Austin, R. Cammi, C. Pomelli, J. Ochterski, R. Martin, K. Morokuma, V. Zakrzewski, G. Voth, P. Salvador, J. Dannenberg, S. Dapprich, A. D. Daniels, O. Farkas, J. B. Foresman, J. V. Ortiz, J. Cioslowski and D. Fox, Gaussian 09, Revision D.01, Gaussian, Inc., Wallingford CT, 2009.

[20] M. McCarroll, S. Yu, S. Harris, S. Puli, I. Kimaru, R. Xu, L. Wang and D. Dyer. *J. Phys. Chem. B.,* 110, (2006), 22991.

[21] (a) J. Zhao, M. Davidson, M. Mahon, G. Kohn and T. James. *J. Am. Chem. Soc*., 126, (2004), 16179. (b) F. Han, L. Feng, X. Liang, S. Ji, S. Liu, F. Zhou, Y. Wu, K. Han, J. Zhao, and T. James. *J. Org. Chem.,* 74, (2009), 1333.

[22] H. Shi, J. Yuan, X. Wu, X. Dong, L. Fang, Y. Miao and F. Cheng. *New J. Chem*., 38, (2014), 2368.

[23] I. Turchi and M. Dewar. *Chem. Rev.,* 75, (1975), 389.

[24] J. Zhong. *Nat. Prod. Rep*., 28, (2011), 1143.

[25] J. Davies. *Tetrahedron*. 60., (2004), 3967.

[26] H. Wasserman, K. Mccarthy and K. Prowse. *Chem. Rev.,* 86, (2009), 845.

[27] (a) T. Gordon, J. Singh and P. Hansen. *Tetrahedron Lett*., 34, (1993), 1901. (b) M. Falorni, G. Dettori and G. Giacomelli. *Tetrahedron Asymmetry*., 9, (1998), 1419. (c) V. Yeh, *Tetrahedron*., 60, (2004), 11995. (d) P. Lv, H. Li, J. Xue, L. Shi and H. Zhu. *Eur. J. Med. Chem.,* 44, (2009), 908.

[28] R. Karimoto, B. Axelrod, J. Wolinsky and E. Schall. *Tetrahedron Lett*., 3, (1962), 83.

[29] W. Crow and J. Hodgkin. *Tetrahedron Lett*., 2, (1963), 85.

[30] S. Naik, J. Harindran and A. Varde. *J. Biotechnol*., 88, (2001), 1.

[31] H. Chobanian, Y. Guo, P. Liu, M. Chioda, S. Fung, T. Lanza, L. Chang, R. Bakshi, J. Dellureficio, Q. Hong, M. McLaughlin, K. Belyk, S. Krska, A. Makarewicz, E. Martel, J. Leone, L. Frey, B. Karanam, M. Maderia, R. Alvaro, J. Shuman, G. Salituro, J. Terebetski, N. Jochnowitz, S. Mistry, E. McGowan, R. Hajdu, M. Rosenbach, C. Abbadie, J. Alexander, L. Shino, K. Sullivan, R. Nargund, M. Wyvratt, L. Lin and R. DeVita. *ACS Med. Chem. Lett*., 5, (2014), 717.

[32] A. Kumar, P. Ahmad, R. Maurya, A. Singh and A. Srivastava. *Eur. J. Med. Chem.*, 44, (2009), 109.

[33] A. Reddy, R. Hymavathi and G. Swamy. *J. Chem. Sci*., 125, (2013), 495.

[34] J. Lee, H. Koh, S. Seo, Y. Baek, H. Rhim, Y. Cho, H. Choo and A. Pae. *Bioorg. Med. Chem. Lett*., 20, (2010), 4219.

[35] Z. Zhong, D. Zhang, Z. Peng, Y. Li, G. Shan, L. Zuo, L. Wu, S. Li, R. Gao and Z. Li. *Eur. J. Med. Chem*., 69, (2013), 32.

[36] C. Wu, Z. Liang, Y. Xu, W. He and J. Xiang. *Chin. Chem. Lett*., 24, (2013), 1064. (b) X. Liu, P. Lv, J. Xue, B. Song and H. Zhu. *Eur. J. Med. Chem*., 44, (2009), 3930. (c) D. Kumar, N. Kumar, S. Sundaree, E. Johnson and K. Shah. Eur. *J. Med. Chem*., 45, (2010), 1244. (d) M. Choi, E. No, D. Thorat, J. Jang, H. Yang, J. Lee, H. Choo, S. Kim, C. Lee, S. Y. Ko, J. Lee, G. Nam and A. Pae. *J. Med. Chem*., 56, (2013), 9008. (e) J. Zhou, J. Jin, Y. Zhang, Y. Yin, X. Chen and B. Xu. Eur. *J. Med. Chem*., 68, (2013), 222. (f) Y. Yamazaki, Y. Kido, K. Hidaka, H. Yasui, Y. Kiso, F. Yakushiji and Y. Hayashi. *Bioorg. Med. Chem. Lett*., 19, (2011), 595. (g) W. Yang, K. Shimada, D. Delva, M. Patel, E. Ode, R. Skouta and B. R. Stockwell. *ACS Med. Chem. Lett.*, 3, (2012), 35.

[37] H. Bredereck and R. Bangert. *Chem. Ber.*, 97, (1964), 1414.

[38] G. Baryshnikov, B. Minaev and V. Minaeva. *Opt Spectrosc*., 110, (2011), 216.

[39] V. Kadam, S. Shaikh and A. Patel. *J. Mol. Struct.*, 1114 (2016), 181.

[40] T. Cynkowski, G. Cynkowska, P. Ashton and P. Crooks. *J. Chem. Soc., Chem. Commun*., 22, (1995), 2335.

[41] O. Dolomanov, L. Bourhis, R. Gildea, J. Howard and H. Puschmann. *J. Appl. Cryst.*, 42, (2009), 339.

[42] L. Palatinus and G. Chapuis. *J. Appl. Cryst*., 40, (2007), 786.

[43] G. Sheldrick. *ActaCryst. A.*, 64, (2008), 112.

[44] A. Khalafi-Nezhad, A. Parhami, M. Rad and A. Zarea. *Tetrahedron Lett*., 46, (2005), 6879.